Sediment Quality Assessment in an industrialized Greek coastal marine area (West Saronikos Gulf)

Georgia Filippi, Manos Dassenakis, Vasiliki Paraskevopoulou, Konstantinos Lazogiannis

Laboratory of Environmental Chemistry Department of Chemistry, National and Kapodistrian University of Athens, Athens, 15784, Greece

Correspondence to: Georgia Filippi (mphilippi@chem.uoa.gr)

Abstract. Eight sediment cores from the coastal marine area of West Saronikos Gulf have been analyzed for grain size and geochemistry. The concentrations of eight metals (Al, Fe, Mn, Cu, Cr, Ni, Pb and Zn) along with total organic carbon (TOC) and carbonate content were measured. The cores are fairly homogeneous, in terms of carbonates and the down-core variability of % TOC, is characterized by high surficial values that decrease with depth. Metal concentrations from both geological (Al, Mn, Cr, Ni) and anthropogenic origin (Cu, Pb, Zn), are higher in the muddy than the sand fraction of sediments. The spatial distribution of Al, Fe, Mn, Cu, Pb and Zn in surface sediments presents increasing concentrations from the northeast to the southwest part of the study area, from the shallow to the deeper parts in contrast to Cr and Ni which are increased in the northern nearshore stations. Based on the vertical distributions, the metal to Al ratios of Cu, Pb and Zn show a constant decrease over depth along most cores, indicating the anthropogenic effects to surface sediments, while Fe/Al is constant. Spearman's correlation analysis performed among the fine grain metal contents, demonstrated a strong positive correlation ($r > 0.5$, $p < 0.05$) between Al, Fe, Mn, Cu , Pb and Zn. The calculated enrichment factors indicate minimal to moderate pollution. The concentrations of Cr at most surface sediments are higher than the ERL value (81 mg Kg^{-1}) but below the ERM value (370 mg Kg^{-1}) and the concentrations of Ni are always higher than the ERM value (51.6 mg Kg^{-1}). In contrast, the concentrations of Cu, Pb, Zn, at most surface sediments, are below ERL values. The mean effects range medium quotients (mERMq) of surface sediments, based on the overall metal concentrations indicated that the surface sediments of most cores, are moderately toxic. The levels of Cr, Ni, Mn and Zn at most stations are decreased in 2017, but the concentrations of Pb and Cu are increased in 2017, compared to a previous study of 2007. The concentrations of Cu, Pb and Zn in the surface sediments of West Saronikos Gulf are lower than levels reported for Inner Saronikos Gulf, Elefsis Bay and other polluted hot spot areas of Greece, owing to a lower degree of urban and industrial development.

1 Introduction

Sediment cores are one of the most easily accessed natural archives, used to evaluate and reconstruct historical pollution trends in aquatic environments. The cores provide data to characterize sediment physical properties and their geochemistry and composition. Vertical profiles of heavy metals can present sedimentation rate, changes in diagenetic processes and evolution of human pressures. Metals released into aquatic systems, undergo several processes, such as adsorption, photolysis, chemical oxidation and microbial degredation. Sedimentation depends on the contaminant physicochemical properties, the sediment physical properties, the adsorption capabilities and the partitioning constant at the water-sediment interface. Trace metals removed from the water column are adsorbed on particulate matter and eventually deposited on bottom sediments (Bigus et al, 2014).

Sediments are repositories for metals such as chromium, lead, copper, nickel, zinc and manganese that present as discrete compounds, ions held by cation-exchanging clays, bound to hydrated oxides of iron and manganese, or chelated by insoluble

humic substances. Solubilization of metals from sedimentary or suspended matter depends on the presence of complexing agents. Metals that are held by suspended particles and sediments are less available than those in true solution (Manahan, 2011).

Saronikos Gulf (Greece) is a marine area of the Aegean Sea between the peninsulas of Attiki and Argolida. The environmental interest in Saronikos gulf arises from the fact that it is the marine border of the most urbanized areas of Greece, i.e., the country's capital (Athens), the industrial zones of Attiki (Elefsis, Thriasio, Sousaki) and the large port city of Piraeus. As a result, there have been on going environmental monitoring and oceanographic studies of Saronikos since the 80's. There are several published works focusing on the eastern part of Saronikos due to the presence of extended and intensive anthropogenic activities (Scoullos, 1986; Pavlidou et al., 2004; Scoullos et al., 2007; Kontogiannis, 2010; Paraskevopoulou et al., 2014; Pangiotoulias et al., 2017; Karageorgis et al., 2020; Prifti et al., 2022). In contrast, fewer studies have focused on North West Saronikos despite the presence of a less extensive industrial zone hosting a major oil refinery and coastal touristic activities along with a particular geological (volcanic/hydrothermal) background (Paraskevopoulou, 2009; Kelepertsis et al., 2001).

The main aim of this work is to assess the levels and the distribution of several heavy metals (Al, Fe, Mn, Pb, Zn, Ni, Cr, Cu) in sediment cores of West Saronikos, in order to discern between the relative contribution of geological and anthropogenic origins and to identify the major sources of metal pollution. The second aim is to determine the evolution of marine pollution in the area by comparing the results with those of a similar study ten years ago, conducted at the Laboratory of Environmental Chemistry (Department of Chemistry, National and Kapodistrian University of Athens). The last aim of this work is to assess and highlight the differences between the concentrations of heavy metals in the surface sediments of West Saronikos in comparison to sediments in studies conducted in East Saronikos, Elefsis bay and other areas of Greece.

2 Study area

Saronikos Gulf is situated at the central Aegean Sea (north east Mediterranean) between $37^0$30'N-$38^0$00'N and $24^0$01' E-$23^0$00' E formed between the peninsulas of Attiki and Argolida. The length of its coastline is 270 km, the surface is 2.866 km^2 and the mean water depth 100 m. To the north, a shallow (30 m depth) embayment is formed, known as Elefsis bay. The islands of Salamina and Aigina and the plateau between them, divide the gulf into two basins: the western basin (Western Saronikos Gulf) with maximum depths of 220 m in the north and 440 m in the south and the eastern basin which has a smooth bathymetry with depths of 50-70 m to the north (Inner Saronikos Gulf) reaching 200 m to the southeast, from where the gulf opens to the Aegean Sea (Outer Saronikos Gulf). To the west, the narrow Isthmus of Corinth connects Korinthiakos Gulf with Saronikos Gulf in the Aegean Sea (Kontoyiannis, 2010; Paraskevopoulou, 2014).

The gulf is subjected to a strong seasonal cycle of heating and cooling, with air temperatures between 0 - 40 ^{o} C, which causes the formation of a seasonal pycnocline from May to November. In winter, the water column is homogenized down to 120 m. However, in the western part, vertical mixing never reached the sea bottom (440 m) in the years after 1992 and dissolved oxygen concentration has approached nearly anoxic conditions (D.O. < 1mL/L) (Paraskevopoulou et al., 2014).

A few circulation studies have been conducted in Saronikos in order to discern the possible movement of the treated wastewater effluent discharged at 65m south of Psittalia island in the eastern basin. The circulation is reported as strongly dependent on local winds with predominant northerly direction throughout the year. However, westerly and southerly winds may also occur in fall, winter and spring. Under the predominant northerly wind regime in summer and fall during the presence of the seasonal pycnocline there is a distinctly different two-layer circulation above and below 60m. In the upper layer there is a general eastward anticyclonic (clockwise) flow from the west to the east basin. Below 60m the flow is reversed from the northeast through the Salamina-Aigina passage to the southwest towards the deeper part of the west basin following a cyclonic (counterclockwise) path. During winter when the water column is fully mixed down to 90m the general flow is anticyclonic from the west to east. Nearshore on the northwest Sousaki coast the currents reported are directed from the north to the south.

In spring during the pycnocline formation there is no continuous flow structure spanning both the west and east basins. In the west during spring there is a rather strong north to south flow (SoHelME, 2005; Kontoyiannis, 2010).

Saronikos gulf, as a whole, is subjected to intense anthropogenic pressure, as it is the marine border of the cities of Athens and Piraeus with 3-4 million inhabitants. Several point and non-point pollution sources are present mainly on the northeastern coasts. One of the most important point sources is the Athens/Pireaus wastewater treatment plant (WWTP) on the small island of Psittalia, among the largest in Europe, with a population equivalent (p.e.) coverage of 5.6 million. Other point sources along the coasts include the port of Piraeus, marinas, touristic facilities, fish farms and the effluents of smaller towns and settlements. Finally, pollution pressure arises from increased marine traffic, since Piraeus is one of the largest and busiest Mediterranean ports, and from the heavy vehicle traffic and the heating systems in the extended urban areas (Paraskevopoulou et al., 2014).

The coastal marine area of the north part of West Saronikos Gulf is affected by a few types of industries established there during the 1970's, that include a major oil refinery unit at the center of Susaki area, a cable manufacturer, soya mills, sulfur / fertilizers manufacturing for agricultural use and the increased sewage load from nearby coastal villages due to the summer tourist season (Kelepertsis et al., 2001; Paraskevopoulou, 2009). The settlements on the coast of West Saronikos, to the best of our knowledge, are not yet connected to wastewater treatment facilities and a projected treatment plant in Aghioi Theodoroi is under construction. The Susaki area, which extends parallel to the northern coast of West Saronikos for about 8 Km, is known for its volcanic activity which took place during Pliocene-Quaternary. Most of the volcanic materials were transported by fluvial processes and deposited in the alluvial plains and coastal regions. The formations observed are peridotites and serpentinites, neogene deposits and Quaternary deposits. As a result, elevated values of Cr, Ni, Co, Mn, Fe are found in the soils and sediments of this area and can be explained by the existence of the ultrabasic rocks (Kelepertsis et al., 2001). The southwest deeper part of West Saronikos (Epidavros basin) could be affected by the transport of organic and inorganic pollutants from the eastern basin due to the periodical northeast to southwest water flow below the pycnocline (Psyllidou-Giouranovits and Pavlidou, 1998; Kontoyannis, 2010).

3. Materials and methods

Eight short sediment cores (12-32 cm) were obtained at corresponding number of stations with varying depths (50-420 m) in the area of West Saronikos Gulf with the use of a box corer. The sampling was conducted on 18 October 2017 with the Greek Oceanographic vessel RV *Aegaeo*. The West Saronikos Gulf study area and the specific location of stations are presented in Fig. 1.

Table 1. Coordinates, water column depth and core length at each sampling station.

Station	Latitude N (dec.minutes)	Longtitude E (dec.minutes)	Depth (m)	Core length (cm)
MOT13A	37^0 54.602	23^0 03.184	50	12
MOT16A	37^0 53.995	23^0 03.080	100	32
UN5	37^0 53.459	23^0 04.393	140	32
MOT16	37^0 54.179	23^0 05. 312	85	20
UN6	37^0 53.455	23^0 10. 857	193	26
UN6A	37^0 51.610	23^0 15.932	165	24
UN4	37^0 57.057	23^0 20.331	79	22
UN11	37^0 38.800	23^0 15.338	420	32

Stations MOT13A, MOT16A, UN5, MOT16, UN6 (near the Susaki area) and UN4 (Megara basin), at the north-western part, are affected by the coastal industrial zone, urbanization and touristic activities. The offshore station UN6A, at the middle of Megara basin, is probably less disturbed by anthropogenic activities. Finally, station UN11, in Epidavros basin at the southwest part of the study area, is influenced by trawling and aquaculture and potential transport of organic and inorganic pollutants from eastern Saronikos due to periodical circulation patterns in the water layers below 60m.

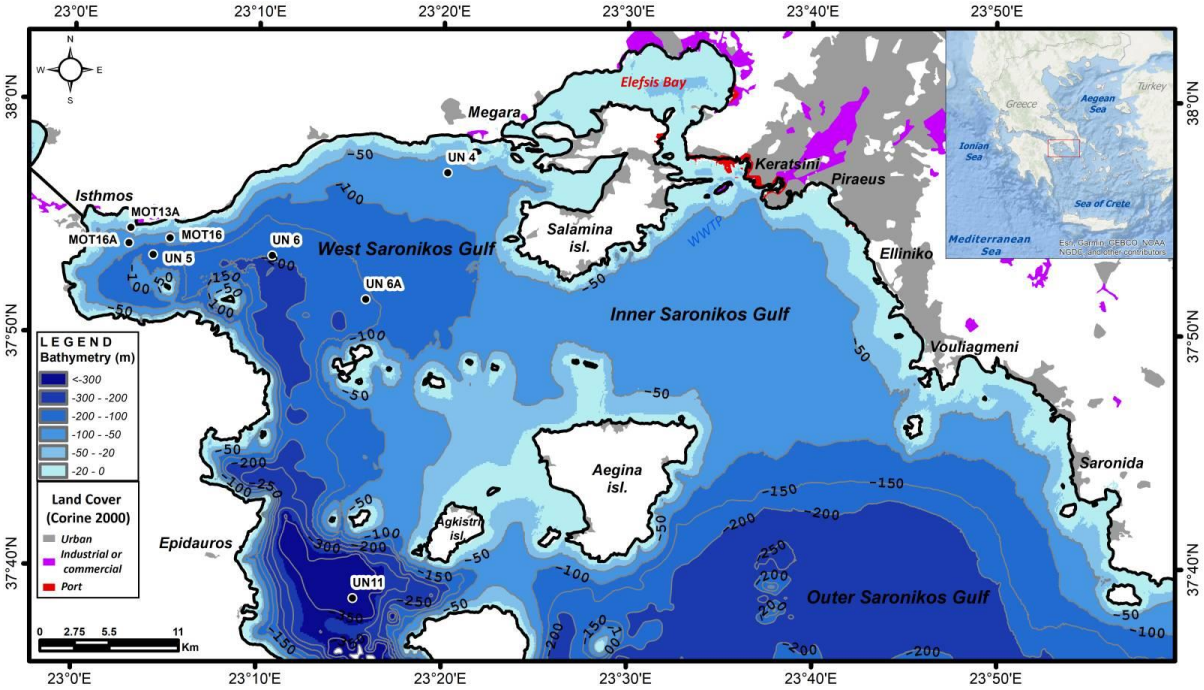

Figure 1: Study area of West Saronikos Gulf and sampling stations (The map was constructed using Arc Map with bathymetry representation data from the European Marine Observation and Data Network-EMODnet: https://portal.emodnet-bathymetry.eu/) and land cover data from Corine 2000).

The cores were frozen immediately after sampling and cut in 1cm layers down to the top 10cm of each core and 2cm layers after that. The separated layers were stored frozen until further processing. The initial step of analysis is removal of water content with the use of a Lab Conco freeze-dryer. Subsequently, grain size analysis via dry sieving was performed using the 1mm and 63μm Retsch stainless steel sieves. The gravel (>1mm), sand (> 63μm) and muddy (<63 μm) fractions were separated for the calculation of the respective percentages to the total sediment. The gravel fraction was discarded. Total organic carbon, carbonates and the concentrations of heavy metals were determined separately in both sand and muddy sediment, when the fraction percentage was more than 10 % of the total sediment or in the prevailing fraction only (above 90%). Table 1 presents the coordinates and depth of each sampling station along with the corresponding core length.

The total organic carbon (TOC) content was measured using the standard Walkley (1947) method as modified by Jackson (1958) and Loring & Rantala (1992), which is based on the exothermic reaction (oxidation) of the sediment with potassium dichromate ($K_2Cr_2O_7$) and concentrated sulfuric acid (H_2SO_4), followed by back-titration with ferrous ammonium sulfate ($FeSO_4$) and ferroine indicator.

The carbonate content was determined by calculating the weight difference of the sample before and after the strong effervescence caused by adding hydrogen chloride (HCl) 6 M to the sediment causing an exothermic reaction followed by HCl gas and CO_2 emission (Loring and Rantala, 1992).

The total metal contents were extracted via complete dissolution of sediment samples with an acid mixture of HNO_3-$HClO_4$-HF (ISO-14869-1:2000) (Peña-Icart et al., 2011). Then, the total metal concentrations were determined by Flame or Graphite Furnace Atomic Absorption Spectroscopy (FAAS-Varian SpectrAA-200 and GFAAS- Varian SpectrAA 640Z) (Skoog et al., 1998). In order to evaluate the precision and accuracy of the method for total metal analysis a certified reference material (PACS-3, NRC-CNRC) was carried through the analytical procedure along with the sediment samples in every digestion batch and 1 or 2 random layers of each core were also analyzed in duplicate. Accuracy was calculated as % recovery (percentage ratio of the measured to the certified value). The precision was evaluated using the % RSD-Relative Standard Deviation (percent ratio of the standard deviation to the average concentration of the replicates) calculated for each metal by each of the duplicate measurements (repeatability estimation) and the multiple measurements of the reference material (reproducibility estimation). The quality data for the total metal method are presented in the Appendix (Table A1). The precision and recoveries

generally fall into the ranges 3-10% RSD and 80-120 % recovery, depending on analyte level. Such results of analytical performance are anticipated for multistage analysis of solid samples and are roughly recommended by the US Environmental Protection Agency (US EPA) and the Association of Official Analytical Chemists (AOAC) (US EPA, 1996; AOAC International, 2016). For every core the %RSD for each metal was calculated as an indication of the downcore variability and the results are presented in Fig. A1 − A15 (Appendix A).

Most statistical treatment of data and the vertical distribution graphs were performed by Microsoft Excel 2010. The horizontal distributions of metals were visualized with the software package Ocean Data View (ODV) 2017. The software IBM-SPSS Statistics 2020 was used for statistical comparisons between stations regarding the trace metal concentrations and Spearman correlation analysis to identify significant relationships between different heavy metals, total organic carbon and carbonates. The comparison between stations was done by performing parametric (One-Way Anova) and non-parametric (Kruskal Wallis, Kolmogorov-Smirnof) tests between the mean values and standard deviations calculated for each metal and each core by the results of the top 5 cm. The comparison between two groups of values, e.g. a variable between two cores or concentrations of variables above-below a certain layer in a single core was either done by two-sided t-test or by the non-parametric equivalents Mann-Whitney and Kolmogorov-Smirnov tests. In all comparative tests statistical results were calculated at the 95% confidence level ($p<0.05$).

4 Results

4.1 Geochemical results

Table 2 summarizes the main findings from the determination of geochemical parameters. The grain size in cores from stations MOT16A, UN5, UN6, UN6A, UN11, is dominated by mud, while the percentage of sand fraction is generally low and below 10% in most core layers. On the other hand, in cores MOT13A, MOT16, UN4 the percentages of both sand (39-66%) and mud (15-50%) are significant. The sediments at stations MOT13A and MOT16 are coarser with average mud percentages 25 and 38% respectively, while at station UN4 especially in the top 10cm the average mud percentage is slightly increased (43%). As a result, the percentages of total organic carbon (TOC) and carbonates as well as the concentrations of heavy metals were determined in the mud fraction (<63μm) of sediments in cores MOT16A, UN5, UN6, UN6A and UN11 and separately in the sand and mud fraction of sediments in cores MOT13A, MOT16 and UN4.

Table 2. Summary statistics of grain size percentages, TOC and carbonate content along the collected cores.

Station	% sand		% mud (silt and clay)		% TOC		% CO_3^{2-}	
	Min	Max	Min	Max	Min	Max	Min	Max
MOT13A	51	66	15	38	0.45	0.92	26	28
MOT16A	1	23	77	99	0.10	0.93	22	23
UN5	1	14	86	99	0.44	1.12	20	23
MOT16	47	65	29	45	0.33	1.28	20	22
UN6	1	32	68	99	0.57	2.44	19	23
UN6A	1	22	78	99	0.33	1.32	22	25
UN4	39	60	20	50	0.51	0.75	29	33
UN11	0	15	74	100	0.77	2.35	15	19

Apart from small variations, the cores are fairly homogeneous, in terms of carbonates. The high percentages of % CO_3^{2-} in cores MOT13A and UN4 are associated with the coarse - grained samples and abundant presence of shell fragments. Figure 2 presents the vertical distribution of % TOC in selected cores. Comparing between stations the lowest TOC values in the top 5cm are measured in the coarser sediments of MOT13A (average 0.57%) and the highest in the deepest station UN11 (average 1.74%). There was no statistical difference between TOC in the remaining cores and the average values for the top 5cm are the following: UN4 (0.68%), MOT16A (0.69%), MOT16 (0.96%), UN5 (0.96%), UN6A (1.09%) and UN6 (1.26%).

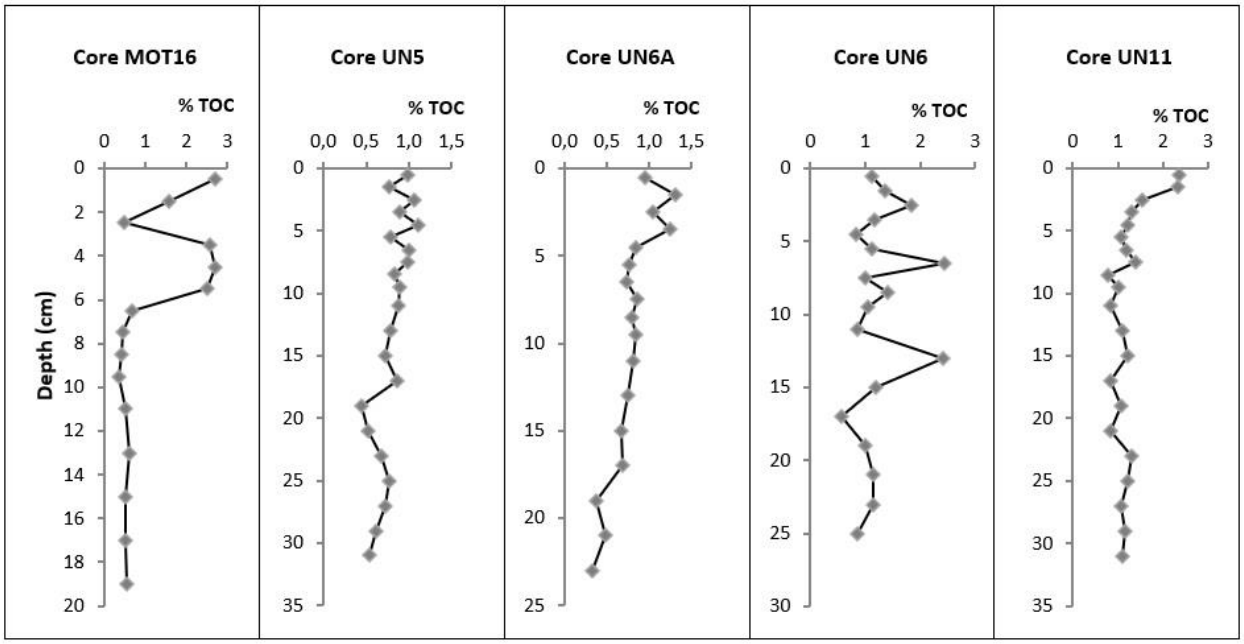

Figure 2: Vertical distribution of % TOC at selected cores [MOT16 profile depicts fine sediment (< 63 μm) TOC content].

The vertical TOC distribution in core MOT16 is differentiated than the corresponding in the adjacent station MOT13A. Below 6cm the levels of TOC are similar in both stations. However, in the top 6cm of core MOT16 average TOC in the total sediment is approximately 1% while below 6cm the corresponding average is 0,42%. This is caused by a striking increase in the TOC content of the muddy sediments, with an average of 2.4% TOC at the top 6cm approximately 5-fold higher than the corresponding in the deeper layers (0.5%). At the same time the TOC variability in the sandy fraction of the top 6cm of MOT16 is minimal, ranging between 0.3% and 0.4%. The vertical TOC distributions of the dominantly muddy cores (MOT16A, UN5, UN6, UN6A, UN11) present high surficial content and gradual increase with depth.

Table 3 presents TOC, carbonate and heavy metal contents in the two fractions (sand-mud) at the shallow coarse-grained cores MOT13A, MOT16, UN4. It is apparent that the % TOC content of the muddy material is higher than the corresponding content of the sandy fraction as anticipated. The % $CaCO_3$ content is increased in the sandy material of cores MOT13A, UN4 compared to that of the fine sediment and is approximately equal in the two sediment fractions of core MOT16.

The concentrations of Al, Cr, Cu, Mn, Pb, Ni and Zn are higher in the muddy sediments of MOT13A and UN4 than the corresponding values in sandy sediments. The same applies to Al, Mn, Cu, and Zn in MOT16. Unlike other metals the Fe content is more or less similar in both sediment fractions of cores MOT13A and UN4. The sediments of core MOT16 appear to be different with higher concentrations of Fe, Cr, Ni and Pb in the coarse-grained fraction.

The vertical distributions of the studied metals in mg kg^{-1} along the collected cores are presented in Figures A1−A15 (Appendix A). In cases of coarse-grained cores MOT13A, MOT16, UN4, the concentrations in the total sediment (calculated by the corresponding values in both fractions) are depicted. Table A2 (Appendix A) presents the ratios of eight heavy metals to Al in the surface and deeper sediment layer of the collected cores. The ratios presented for the cores MOT13A, MOT16, UN4 are calculated by the results in the corresponding fine-grained sediments. The vertical profiles of metal to aluminum ratios (in fine grained sediments) along the collected cores, are also given in Figures A1−A15 (Appendix A).

Table 4 summarizes the concentrations of eight heavy metals in the surface and deeper sediment layer of the collected cores. For the sake of direct comparison in the cases of cores MOT13A, MOT16, UN4 the fine grained concentrations are presented in Table 4. The sediments at the deeper parts of West Saronikos (cores UN6, UN6A and UN11) present elevated concentrations of Al, Fe, Pb and Zn. The sediments of UN11 are also particularly enriched in Mn. On the contrary the values of Cr and Ni are elevated in cores MOT13A, MOT16 and MOT16A.

Table 3. Concentrations of metals (in mg Kg^{-1}), organic and inorganic carbon content in the two sediment fractions of coarse-grained cores (MOT13A, MOT16, UN4).

Variable/Core	MOT13A		MOT16		UN4	
	fine fraction	coarse fraction	fine fraction	coarse fraction	fine fraction	coarse fraction
% TOC	0.64-2.80	0.26-0.45	0.37-2.70	0.15-0.46	0.65-0.94	0.43-0.58
% $CaCO_3$	22-23	27-30	21-23	18-22	26-29	32-36
Al	10561-18387	6615-9226	21677-28939	10610-18538	23271-34246	10449-19765
Cr	390-651	333-486	322-374	306-517	113-133	71.6-115
Ni	293-411	220-302	314-573	424-697	139-187	78.0-140
Fe	19878-21153	17430-20643	24130-31694	32265-36080	14149-17126	13501-17931
Mn	429-476	326-386	471-530	435-484	317-366	174-238
Cu	17.1-18.8	8.9-11.8	16.7-22.6	6.7-14.8	15.1-23.6	9.7-13.4
Pb	18.0-30.7	14.8-21.0	9.1-28.0	8.3-31.9	11.2-31.2	9.3-27.3
Zn	39.3-51.8	31.0-45.6	39.8-53.7	31.5-50.9	38.9-59.2	30.3-50.3

Table 4. Concentrations in mg Kg^{-1} of metals in the surface and the deeper sediment layer of cores. The concentrations at coarse-grained cores MOT13A, MOT16, UN4 refer to the fine sediment fraction (f < 63μm).

Core	Layer (cm)	Al	Cr	Ni	Fe	Mn	Cu	Pb	Zn
MOT13A	0-1	10561	651	411	20988	476	18.2	26.1	49.6
	10-12	14673	407	383	21153	444	18.1	22.5	44.6
MOT16A	0-1	27009	280	375	23315	578	22.6	20.4	48.3
	30-32	30070	256	382	26179	562	22.1	28.1	44.1
UN5	0-1	32705	199	305	25534	635	27.4	42.7	74.5
	30-32	37885	223	320	29170	520	26.0	24.7	57.5
MOT16	0-1	21677	369	377	25816	530	22.6	28.0	53.7
	18-20	23807	348	401	29752	482	16.9	9.1	40.4
UN6	0-1	43264	142	253	27301	954	36.7	52.9	92.1
	24-26	44547	153	274	29345	707	28.5	32.5	62.4
UN6A	0-1	39314	146	187	21838	570	26.3	38.4	73.8
	22-24	41303	161	209	23827	513	25.4	38.7	58.7
UN4	0-1	34246	132	162	15762	358	23.6	26.1	52.1
	20-22	31706	113	160	17112	365	15.1	12.0	40.3
UN11	0-1	54626	142	230	32177	3925	49.7	63.9	110
	30-32	48186	163	217	31573	1459	37.3	35.1	71.4

The vertical distributions of Al (Fig. A1) for the total sediment (both fractions) present minimal variation. The down-core variability of Al is lower than 10 %, in the finer sediments (MOT16A, UN5, UN6, UN6A and UN11) and between 10-15 % in the coarser sediments (MOT13A, MOT16 and UN4). In the surface layer (0-1cm) of cores MOT13A and UN5 there is a sharp decrease of Al content. Furthermore, the average aluminum content (16709mgKg^{-1}) at the top 6cm of core MOT16 is statistically lower (two-sided t-test, p<0,05) than the corresponding average content in the layers below (20477mgKg-1). On the contrary, at the top 12cm of core UN11 aluminum (average 52714mgKg^{-1}) is increased (two-sided t-test, p<0,05) compared to the deeper layers (average 48621 mgKg^{-1}). The other so-called lithogenic metals (Cr, Ni, Fe, Mn) generally present uniform vertical profiles with minimal variability, mostly below 10 % (Figures A2-A9). However, Cr, Ni, Fe and Mn in the surface sediments of MOT13A present an increasing trend, that remains pronounced after normalization to Al in the muddy fraction at the top 0-1cm and is concurrent with the 2-fold decrease of Al content. The vertical profiles of Cr and normalized Cr/Al in UN11 indicate a decrease of Cr in the upper sediment layers. This decrease is confirmed statistically and the average Cr (148mgKg^{-1}) and Cr/Al (28,0) values of the top 12cm are lower than the corresponding in the deeper layers (155 mg$Kg^{-1}$and 32,0, respectively). The same trend of decrease in the top 0-1cm is seen in the normalized profiles of Fe, Ni and Mn in the fine-grained sediment fraction of core UN4. The average concentrations of Fe, Mn, and Ni in the top 12cm of UN11 are statistically higher than the corresponding in the deeper layers. The most pronounced difference is calculated for Mn, where the average upper layer content is 2396 mgKg^{-1} while the deeper layer content is 1527 mgKg^{-1}. The same applies to Mn/Al ratio in UN11 but not to the ratios of Fe/Al and Ni/Al which are seemingly lower in the upper layers like Cr/Al but statistically equal. The down-core variability of Mn in all stations, except UN4, is typical of shelf sediments, with high surficial Mn concentrations and Mn/Al ratios that diminish with depth

Figure 3 presents selected vertical profiles of Mn and Pb along core UN11 and those of Cr, Fe, Cu, Zn at stations UN6A, MOT16A, UN4, UN6, respectively. Figure 4 presents selected vertical distributions of metal to Al ratios at cores MOT13A, UN5, MOT16A, MOT16 and UN11. The concentrations and ratios presented in Figures 3 and 4 refer to the muddy fraction of the sediments in the cases of the coarse-grained cores (MOT13A, MOT16, UN4).

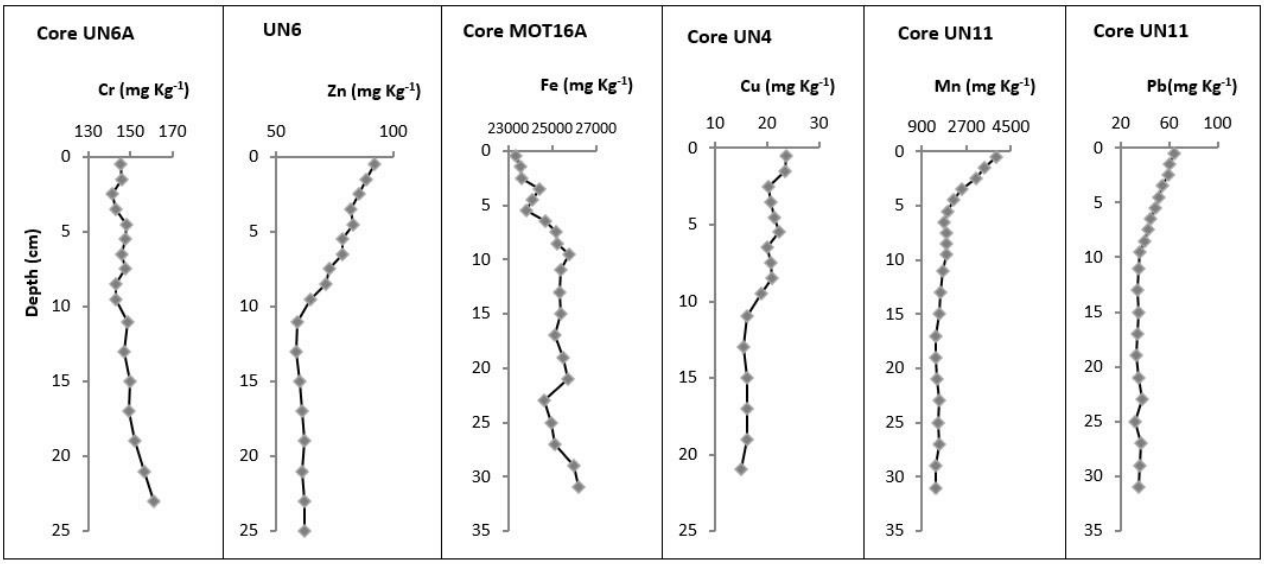

Figure 3: Vertical profiles of Cr, Fe, Cu, Zn at the muddy sediments of cores UN6A, MOT16A, UN4, UN6 respectively and Mn, Pb along core UN11.

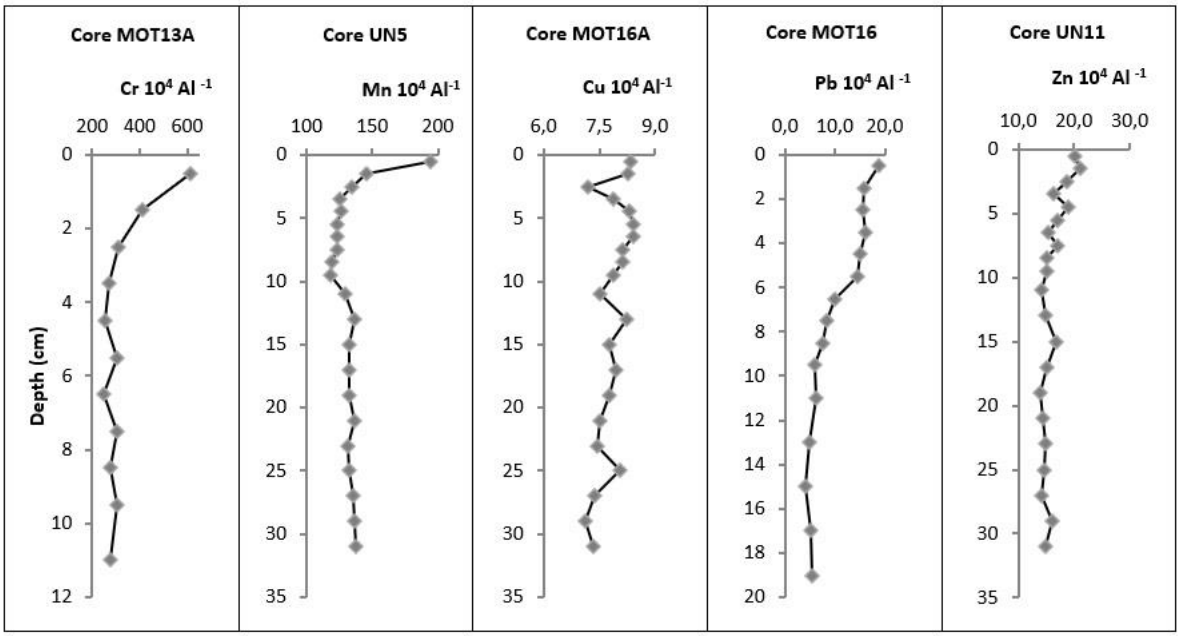

Figure 4: Vertical distributions of ratios to Al at cores MOT13A, UN5, MOT16A, MOT16 and UN11 of northwest Saronikos Gulf (profiles for MOT13A and MOT16 depict ratios calculated for the muddy fraction).

The concentrations of Cu, Pb and Zn as well as the normalized profiles (Fig. A10−A15) show a constant decrease over depth to background levels. That tendency is less pronounced with no statistical difference between upper and deeper sediment layers in very few cases and particularly for Cu (MOT13A, MOT16, MOT16A), Cu/Al (MOT13A), Pb (MOT13A, MOT16A), Pb/Al (MOT16A) and Zn (MOT16A). In all remaining cores the concentrations of Cu, Pb and Zn and the ratios to aluminum in the upper sediment layers (above 10cm) are statistically higher than the corresponding in the deeper layers.

4.2 Horizontal distributions

Figure 5 presents the horizontal distributions of heavy metals in the surface sediments (0-1 cm) of the study area. In cases of coarse surface sediments of MOT13A, MOT16, UN4, the concentrations of total sediment fraction (sand and mud) were used. The concentrations of Al, Fe, Mn, Cu, Pb and Zn are plotted increased from the northeast to the southwest area of West Saronikos Gulf. On the other hand, the concentrations of Fe, Cr and Ni at the north part appear higher than those at the south area.

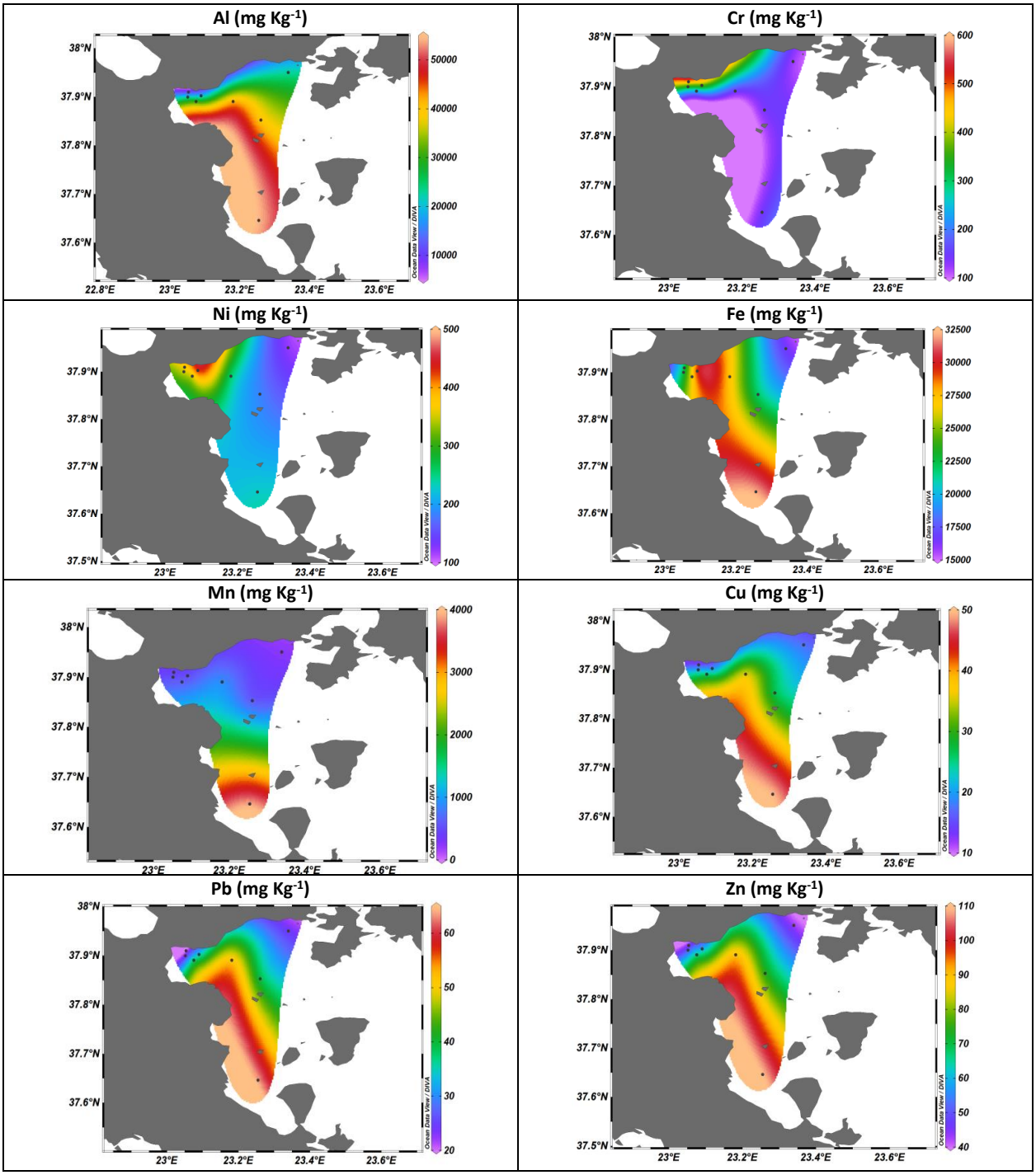

Figure 5: The horizontal distributions of heavy metals in the surface sediments of West Saronikos Gulf. In cases of coarse surface sediments of stations MOT13A, MOT16, UN4, the concentrations of the total sediment (sand and mud) were used.

In order to corroborate the above plots and produce solid statistical comparisons for the metal concentrations between stations the average values and standard deviation from the results of the top 5 cm were calculated and examined used the IBM-SPSS

Statistics 2020 software. In most cases of metals and stations the 5 value groups followed the normal distribution therefore the parametric One-Way Anova test was first applied. But since some cases did not follow the normal distribution non-parametric tests (Kruskal-Wallis for multiple groups and Mann-Whitney / Kolmogorov-Smirnov for two groups) were also applied to corroborate the statistical comparison outcome. The results summary is the following:

Al: UN11 >> UN6 = UN6A > UN5 > MOT16A > UN4 = MOT16 >> MOT13A

Fe: UN11 = MOT16 > UN6 = UN5 >MOT16A > MOT13A=UN6A > UN4

Mn: UN11 >> UN6 > MOT16A = UN6A = UN5 = MOT16 > MOT13A > UN4

Cr: MOT13A = MOT16 > MOT16A > UN5 > UN6A = UN11 = UN6 > UN4

Ni: MOT16 > MOT16A > UN5 = MOT13A = UN6 > UN11 > UN6A > UN4

Cu: UN11 > UN6 = UN5 > UN6A > MOT 16A > UN4 = MOT16 > MOT13A

Pb: UN11 = UN6 > UN5 = UN6A > UN4 = MOT16 > MOT 16A = MOT13A

Zn: UN11 > UN6 > UN5 = UN6A > MOT16 = UN4 = MOT 16A = MOT13A.

5 Discussion

5.1 Geochemical findings and element interrelations

The spatial grain size distribution falls into an expected pattern with coarser sediments closer to the coastline (stations MOT13A, MOT16, UN4) and finer sediments in the more remote and deeper stations MOT16A, UN5, UN6, UN6A, UN11.

The observed spatial variability of TOC with higher content in the predominantly muddy cores is expected since fine-grained sediments are known to contain elevated levels of organic material compared to coarse-grained sediments (Salomons & Forstner, 1984). The pronounced increase of TOC in the muddy sediments of station MOT16 (top 6cm) could be attributed to the treated wastewater effluents of the refinery which are discharged in the general vicinity of this station (Paraskevopoulou; 2009). The two deep stations UN6 (200m at Megara basin) and UN11 (440m at Epidavros basin) present the highest TOC content. It has been stipulated that suspended matter from eastern Saronikos basin, which is affected by more pronounced polluting activities is transported below the thermocline to the west basin (Psyllidou-Giouranovits and Pavlidou, 1998; Kontoyannis, 2010). This could explain the gradual increase of TOC content in the more recently deposited upper layers of sediment.

Fine-grained sediments are known to contain abundant geochemical phases, such as clay minerals, organic material and Fe-Mn oxy-hydroxides with high affinity for trace metals due to increased surface adsorption and ionic attraction. Thus, the elevated levels of Al and the so-called anthropogenic metals (Cu, Pb, Zn) in the muddy sediments of the study area can be attributed to the predominant occurrence of aluminum-rich aluminosilicate and clay minerals in fine-grained sediments and their concurrent efficacy to bind or sorb trace metals (Barjy et al., 2020; Karageorgis et al., 2005; Salomons & Forstner, 1984). In contrast Cr and Ni which are also regarded as lithogenic elements along with Al, present a different distribution and are elevated in the coarser near-shore sediments of cores MOT13A, MOT16 and MOT16A. This can be attributed to the existence of ultrabasic rocks in the coastal Susaki area, in which, these metals are abundant (Kelepertsis et al., 2001). In the case of Fe and Mn the lower contents at station UN4 can be attributed to the coarser sediments and the different geological setting with absence of ultrabasic rocks.

The minimal depth variations observed at the vertical distributions of major (Al) and lithogenic elements (Fe, Cr, Ni) in the study area are anticipated because of their terrigenous origin (Nolting et al., 1999; Karageorgis et al., 2005;), however some of the discrepancies identified in specific cores cannot be readily explained due to lack of data for other elements such as Ti, Si and Ca.

The down-core variability of Mn in all stations, except UN4, is typical of shelf sediments, with high surficial Mn concentrations that diminish with depth, as reducing conditions develop. These variations are largely independent of lithological or carbonate

content fluctuations, and are attributed solely on the respiration of organic carbon and the redox-cycle of Mn (Karageorgis et al., 2005; Sundby, 2006). The Mn enrichment is far more pronounced in the surface sediments of station UN11 and subtle in the other muddy cores. In station UN11 the bottom waters have been hypoxic or near anoxic since the mid 90's (Kontoyiannis, 2010; Paraskevopoulou et al., 2014). A possible explanation is that the slow diffusion of dissolved oxygen from the more oxidizing overlying waters and the upward diffusion of dissolved Mn (II) from the pore water of anoxic surface sediments to the sediment/water interface (Ozturk, 1995), cause the oxidation of dissolved Mn (II) and its precipitation as Mn (IV) oxides (Pohl and Hennings, 1999). The Mn enrichment in the surface layers of UN11 resembles concentrations in sediments from suboxic parts of the Black Sea (Kiratli & Ergin, 1996; Chen et al., 2022).

The normalized profiles of Cu, Pb and Zn exhibit statistically higher metal ratios in the upper layers of the cores, which is a typical indication of the effect of modern pollution sources to recently deposited sediments in contrast to pre-industrial deposition of the deeper layers (Karageorgis. et al., 2005).

The concentrations of Al, Fe, Mn, Cu, Pb and Zn are increased from the northeast to the southwest area of West Saronikos Gulf generally following the distribution of muddy sediments. The opposite increase of Cr and Ni to the north of the study area is attributed to the ultrabasic geological substrate of the Susaki coastal area. The exception of increased Fe concentrations in one of the northern sandy cores (MOT16) can also be attributed to the geology of the coastal region (Kelepertsis et al., 2001).

Spearman's correlation analysis was carried out to determine the relationships between heavy metals and percentages of total organic carbon (TOC) and carbonates in sediments of the collected cores. The concentrations of metals and the percentages of organic and inorganic carbon used for the analysis correspond to the fine fraction in the sediments of stations MOT13A, MOT16, UN4. Spearman's correlation coefficients are presented in Table A3 (appendix A) and Fig. A16 (appendix A).

Al is highly correlated ($r > 0.5$, $p < 0.05$) with Fe, Mn, Cu, Pb and Zn, which probably indicates an association between these metals in the form of metal-clay complexes of continental origin (Barjy et al., 2020). On the other hand, there is a negative correlation of Al with Cr and Ni.

Cr is highly correlated with Ni, but both of them show negative correlation with Cu, Pb and Zn, which can be attributed to their different origin (Barjy et al., 2020) and poor correlation with Mn. Cr shows poor correlation with Fe, as well. The strong correlation between Cr and Ni can be observed at sediments of the northwest part, too.

Fe, Mn, Cu, Pb and Zn show positive correlation with each other. Cu, Pb and Zn are highly correlated with each other ($r > 0.5$, $p < 0.05$), which can be observed at sediments of the northwest part, too, suggesting that they have a common origin and identical behavior during transport in the marine environment (Barjy et al., 2020).

The % TOC content presents moderate correlation with Al, Cu, Pb and Zn and negative correlation with Cr, Ni and % carbonates. Moreover, it shows poor correlation with Fe and Mn. Finally, the percentage of carbonates content presents negative correlation with all metals.

5.2 Enrichment Factors

The Enrichment Factors (EF) are used to distinguish between metals originating from anthropogenic activities and from natural processes, assessing the degree of anthropogenic effect. Equation (1) was used for the calculations of EFs, where C_x is the concentration of the analyzed metal and C_{EN} is the concentration of the normalizing element. Al was used as the reference element.

$$EF = (C_x/C_{EN})_{sample}/(C_x/C_{EN})_{background} \quad (1)$$

In Table 5, the categories of contamination according to the Enrichment Factor are presented (Diamantopoulou et al., 2019; Sutherland, 2000). In general, EFs use concentrations normalized to Al to account for the heterogeneity of the samples due to differences in texture and organic content (Gredilla et al., 2015).

Table 5. The categories of pollution according to the Enrichment Factor.

EF	Contamination Degree
< 2	Depletion to minimal enrichment- no or minimal pollution
2 to 5	Moderate enrichment- moderate pollution
5 to 20	Significant enrichment- significant pollution
20 to 40	Very high enrichment- very strong pollution
>40	Extreme enrichment- extreme pollution

Table 6 presents the Enrichment Factors of the surface sediments (0-1 cm) that were calculated based on the measured concentrations of heavy metals. The EFs were calculated at the fine fraction (f < 63μm) of sediments of cores MOT13A, MOT16, UN4. Most metals present minimal to moderate enrichment in almost all the cores analysed. Moderate enrichment is found for Cr, Ni, Mn and Pb in core MOT13A, Mn in UN11, and finally for Pb in UN5 and MOT16.

Table 6. Enrichment Factors of the surface sediments (0-1cm) of the study area. In cases of stations MOT13, MOT16, UN4, the EFs were calculated at the fine surface sediment fraction (f < 63μm).

Core	EF Cr	EF Ni	EF Fe	EF Mn	EF Cu	EF Pb	EF Zn
MOT 13 A	3.09	2.07	1.92	2.07	1.94	2.24	2.14
MOT 16A	1.36	1.22	1.10	1.27	1.27	0.90	1.36
UN 5	1.20	1.28	1.17	1.64	1.42	2.32	1.74
MOT 16	1.28	1.14	1.05	1.33	1.61	3.71	1.60
UN6	0.98	0.98	0.99	1.43	1.36	1.73	1.57
UN 6A	1.00	0.99	1.01	1.23	1.15	1.09	1.39
UN 4	1.00	0.87	0.79	0.84	1.34	1.86	1.11
UN11	0.68	0.82	0.79	2.09	1.04	1.42	1.20

5.3 Sediment Quality Guidelines

Sediment Quality Guidelines (SQG) of effects range low (ERL) and effects range median (ERM) are used to assess the level of toxicity of metals in the surface sediments. Metal concentrations below the ERL value, indicate that effects on biota are rarely observed. Concentrations above the ERL but below the ERM, occasionally affect the biota and concentrations above the ERM frequently affect the biota. The ERL and ERM guideline values for trace metals ($mfKg^{-1}$, dry wt) and percent incidence of biological effects in concentrations ranges defined by the two values are presented in Table 7 (Long et al., 1995).

Table 7. ERL and ERM guideline values for trace metals ($mgKg^{-1}$, dry wt) and percent incidence of biological effects in concentration ranges defined by the two values.

Metal	ERL (mg kg^{-1})	ERM (mg kg^{-1})	Percent incidence of effects		
			<ERL	ERL-ERM	>ERM
Cr	81	370	2.9	21.1	95.0
Cu	34	270	9.4	29.1	83.7
Pb	46.7	218	8.0	35.8	90.2
Ni	20.9	51.6	1.9	16.7	16.9
Zn	150	410	6.1	47.0	69.8

In this study, the concentrations of heavy metals at the surface sediments were compared with the ERL and ERM criteria. For cores MOT13A, MOT16, UN4, the concentrations in the total sediment (< 1mm) were used. The concentrations of Cr in the surface sediments of cores UN4, UN5, MOT16A, UN6, UN6A and UN11 are higher than the ERL value (81 mg Kg^{-1}) but below the ERM value (370 mg Kg^{-1}) and the values at surface sediments of MOT13A and MOT16 are higher than the ERM value. The concentrations of Ni at the surface sediments of the collected cores are higher than the ERM value (51.6 mg Kg^{-1}) and as a result, they frequently affect the biota (Long et al., 1995; Hahladakis et al., 2012).

The concentrations of Cu and Pb at surface sediments of stations MOT13A, MOT16A, UN4, UN5, MOT16 and UN6A, are below the ERL values (34 mg Kg^{-1} for Cu and 46.7 mg Kg^{-1} for Pb), which indicates that effects on biota are rarely observed. On the other hand, the concentrations at surface sediments of cores UN6 and UN11 are higher than the ERL values but below

the ERM values (270 mg Kg^{-1} for Cu and 218 mg Kg^{-1} for Pb), which means that they can occasionally affect biota . The concentrations of Zn are below the ERL (150 mg Kg^{-1}) value and the ERM value (410 mg Kg^{-1}), which indicates that effects on biota are rarely observed (Long et al., 1995; Hahladakis et al., 2012).

5.4 Mean effects range medium quotients

The mean effects range medium quotient (mERMq) is an index that is used to evaluate the possible biological effects of the coupled toxicity of all heavy metals in the surface sediments (Gredilla et al., 2015). Briefly, mERMq's were calculated by dividing the average concentration of each metal at the top 9cm, by its respective ERM (effects range median), to obtain the corresponding sediment quality guideline quotient (ERMq). Following this, mERMq's for each core were obtained as the average of ERMqs previously calculated. ERMqs indicate the pollutant concentration above which effects are expected to be frequent and have been only defined for very toxic elements (Gredilla et al., 2015).

In this study, Cr, Ni, Cu, Pb and Zn were considered in our calculations and the results are depicted in Table 8. In cases of cores MOT13A, MOT16, UN4, the concentrations of the total sediment (< 1mm) were used for the calculation of mERMq. Values of mERMq in the ranges of 0.0-0.1, 0.1-0.5, 0.5-1.5 and >1.5 correspond to the following probabilities of toxicity: 9 % (non-toxic), 21 % (slightly toxic), 49 % (moderately toxic) and 76 % (highly toxic), respectively (Gredilla et al., 2015). The mERMq values obtained for the sediments varied from 0.62 to 2.00, which means that the sediments are moderately or highly toxic.

The concentrations of Cr, Ni, Cu, Pb, Zn in sediments of cores MOT13A, UN5, UN6, UN6A, UN4 and UN11 are moderately toxic and in sediments of MOT16A and MOT16 highly toxic. The concentrations of Cu, Pb, Zn in sediments of cores MOT13A, MOT16A, MOT16, UN4 are non-toxic, with mERMq ranging from 0.08 to 0.10 and those in sediments of UN5, UN6, UN6A, UN11 are slightly toxic, with mERMq range 0.16-0.21.

Table 8. MERMqs values calculated for the surface sediments (0-9 cm) of the collected cores of West Saronikos Gulf, by dividing the average concentration (mg Kg^{-1}) of each metal (Cr, Ni, Cu, Pb, Zn) by its respective ERM (mg Kg^{-1}). In cases of cores MOT13A, MOT16, UN4, the concentrations of total sediment (< 1mm) were used.

Core	mERMq (average)	toxicity of sediments
MOT13A	1.46	Moderately toxic
MOT16A	1.69	Highly toxic
UN5	1.46	Moderately toxic
MOT16	2.00	Highly toxic
UN6	1.21	Moderately toxic
UN6A	0.95	Moderately toxic
UN4	0.62	Moderately toxic
UN11	1.09	Moderately toxic

5.5 Evolution of marine pollution

The total concentrations of eight heavy metals in the surface sediments were compared with those of a similar study ten years ago (Paraskevopoulou, 2009). In cores MOT13A, MOT16, UN4, the concentrations of the total sediment fraction (<1mm) were used and the results are depicted in Fig.6. The levels of Cr, Ni and Mn at most sediments, are decreased in 2017, compared to the study of 2007. On the other hand, the levels of Pb and Cu are increased in 2017, compared to the study of 2007. Moreover, the levels of Zn, at most sediments, are decreased in 2017 compared to the study of 2007.

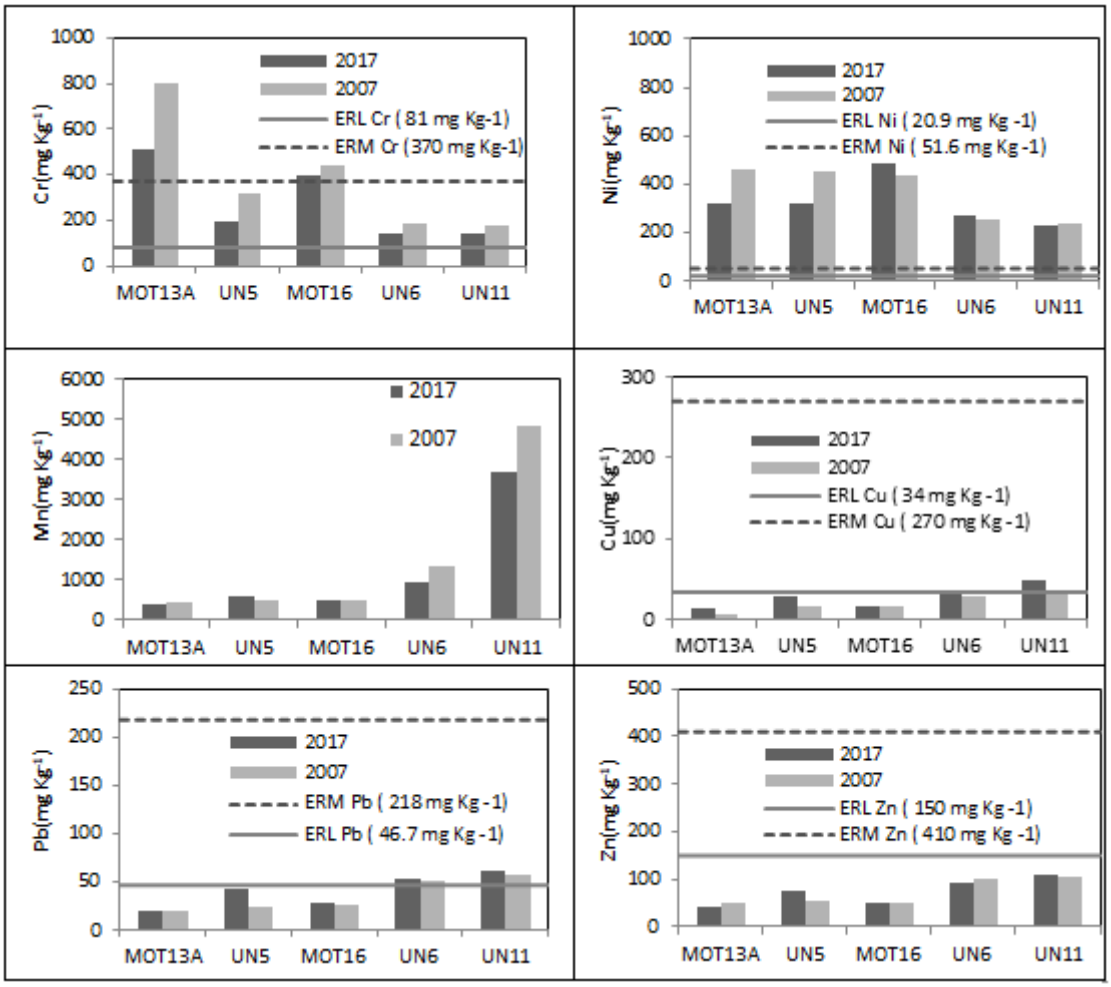

Figure 6: Levels of heavy metals in surface sediments of 2017 and 2007 plotted with sediment quality guidelines. For the coarse sediments of stations MOT13A, MOT16, UN4, the concentrations of total sediment (< 1mm) were used.

5.6 Comparison of metal concentrations in West Saronikos Gulf with other areas of Saronikos Gulf

The concentrations of heavy metals in the surface sediments of West Saronikos Gulf from the present study are compared with data from the other sub-areas of Saronikos. Specifically the data reviewed are: a) from surface sediments collected in Elefsis Bay (EB), Inner Saronikos Gulf (ISG) and Outer Saronikos Gulf (OSG) during the same sampling of October 2017 and analyzed in the Laboratory of Environmental Chemistry using the same methodologies (Xarlis; 2018; Vrettou,2019) and b) data from surface sediments in Elefsis Bay (EB), Inner Saronikos Gulf (ISG) and Outer Saronikos Gulf (OSG) from various samplings conducted by the Hellenic Centre for Marine Research and analyzed by X-ray Fluorescence (Karageorgis et al., 2020; Karageorgis et al., 2020a). Summary results of this comparative review are provided in Table 9. The location of selected stations from the other sub-areas of Saronikos are roughly given in Fig. A17 (Appendix). Furthermore, metal concentrations in sediments from various areas of Greece analyzed by X-ray Fluorescence (Kanellopoulos et al., 2022) were also reviewed. It is observed that high Al concentrations are recorded at West Saronikos as well as the Outer Gulf, related to the settling of finer aluminosilicates in deeper waters. Moreover, high values of Al contents at Elefsis Bay (S1 and neighbouring stations, Fig. A17) are attributed to the terrigenous inputs from ephemeral streams discharging into the bay (Karageorgis et al., 2020). Cr and Ni contents show maxima in the northwestern stations (MOT13A, MOT16, MOT16A) offshore Susaki, due to the geological contribution from ophiolite complexes (Kelepertsis et al., 2001). Ni and Cr concentrations throughout the northwest area of Saronikos are higher than the mean background contents (117 mg Kg^{-1} for Ni and 142 mg Kg^{-1} for Cr) estimated from sediments sampled at various areas of Greece and similar to concentrations reported for Aliveri Bay and the Asopos river basin, also related to occurrence of ultrabasic rocks (Kanellopoulos et al., 2022).

The concentrations of Mn and Fe are similar throughout the sub-areas of Saronikos Gulf, with the exception of Epidavros basin, where the maximum values are recorded due to the settling of finer aluminosilicates in deeper waters and possibly the implications of bottom water hypoxia/anoxia already discussed in previous sections (Kontoyannis, 2010; Karageorgis et al., 2020).

Table 9. Comparison of heavy metals concentrations in mg Kg^{-1} between areas of Saronikos Gulf.

Area / Stations	Al	Cr	Ni	Fe	Mn	Cu	Pb	Zn	References
West Saronikos									Present work
MOT13A, MOT16, MOT16A	5697-27009	280-552	344-484	20740-21191	422-578	13.5-22.6	20.0-30.3	44.1-52.1	
UN5, UN6, UN6A	32705-43264	142-199	187-305	21838-27301	570-954	26.3-36.7	38.4-52.9	73.8-92.1	
UN4	22702	123	123	16682	270	17.5	24.5	43.6	
UN11	54626	142	230	32177	3925	49.7	63.9	110	
Outer Saronikos	14000-42000	81.5-133	29.5-106	6407-27139	293-1159	12.8-22.9	15.9-58.9	32.4-110	Karageorgis et al., 2020a; Vrettou,2019
Inner Saronikos	2900 37700	30.7-184	9.6-87.1	3235-20795	61.5-442	7.9-68.5	8.2-73.6	15.2-170	Karageorgis et al., 2020a; Vrettou, 2019; Xarlis,2018
Psitatalia (S7)	26780	-	83.2	20623	239	103	102	251	Panagopoulou, 2018; Xarlis, 2018
Elefsis Bay	35000 61000	108-176	41.2-119	29721-30499	282-579	32.1-137	61.0-171	188-521	Karageorgis et al., 2020a; Xarlis,2018

The so-called anthropogenic metals Cu, Pb and Zn show maxima at Elefsis Bay, while their concentrations at the other parts of Saronikos are reported lower. The levels at Epidavros basin (UN11) are the highest among the stations of West Saronikos, which can be attributed to the transport of pollutants from the eastern basin (Psyllidou-Giouranovits and Pavlidou, 1998; Dassenakis et al., 2003). However, the West Saronikos levels of Cu, Pb and Zn remain lower than polluted stations of Inner Saronikos, such as OS2 (near the port of Pireaus) and S7 (Psittalia, outfall of the Athens Waste Water Treatment Plant) presented depicted in Gig. A17. Furthermore, Cu, Pb and Zn concentrations at Megara and Epidavros basins are similar to those at surface sediments of Malliakos and Pagassitikos Gulf (Kanellopoulos et al., 2022) and the concentrations found in most stations of Inner and Outer Saronikos (Karageorgis et al., 2020; Panagopoulou,2018; Vrettou,2019; Xarlis,2018) but higher than less affected island areas such as Chios Port, Milos and Andros (Kanellopoulos et al., 2022). In general the West Saronikos sediments, affected by a relatively small industrial zone, are much less contaminated by Zn compared to the concentrations well above 150 mg Kg^{-1} found in specific locations of Elefsis Bay, Inner Saronikos, Thessaloniki Bay, Ierissos and Lavrio (Karageorgis et al., 2020, Kanellopoulos et al., 2022) with extensive pollution sources such as the Elefsis industrial zone, Piraeus Port, the Athens Waste Water Treatment Plant outfall, major rivers of Northern Greece and current or historical mining operations.

6 Conclusions

The heavy metal pollution of West Saronikos Gulf has not been sufficiently studied, despite the scientific interest of this area, in contrast to the numerous studies of the eastern coast. The distribution of metals in the sediment samples of West Saronikos indicates that the area is enriched in metals from both geological and anthropogenic origins. The concentrations of all metals (Al, Mn, Cr, Ni, Cu, Pb, Zn) im muddy sediments are higher than those measured in sandy sediments. The cores are fairly homogeneous, in terms of carbonates and the down-core variability of % TOC, is characterized by high surficial values that decrease with depth.

The Cr and Ni concentrations at the northwest part of the study area are higher than those measured at the southwest area and their values are very stable with depth of most sediment cores, which can be attributed to the geological background of the adjacent coast. Al, Fe and Mn are increased from the northeast to the southwest part of the study area. The concentrations of

Al and Fe increase with depth in most cores, while the values of Mn decrease with depth. Generally, concentrations of Fe and Mn at surface sediments are affected by oxic and hypoxic conditions and the settling of finer aluminosilicates.

The vertical distributions of Cu, Pb and Zn present a constant decrease over depth along most cores, which can be attributed to their anthropogenic origin. Moreover, their levels at most sediments are higher than those measured ten years ago. Finally, the Cu, Pb, Zn concentrations in West Saronikos Gulf surface sediments are comparable with those at Outer Saronikos Gulf and lower than those from Inner Saronikos Gulf, Elefsis Bay and other pollution hot spots of Greece, which can be attributed to the smaller industrial zone and sparce urbanized settlements of the West Saronikos coast.

The concentrations of metals that are measured higher than the ERL values and the indication for moderately or highly toxic sediments by the calculation of mERMq signify that more research is required, in order to investigate probable effects on the marine ecosystem. Continuous monitoring, updating of the results of the present study complemented with detailed geochemical analysis for major elements and minerals identification as well as core dating, metal speciation and study of bioaccumulation should be conducted, to assess the impacts of heavy metal pollution on the marine environment of West Saronikos Gulf.

7 Appendices

Appendix A

Table A1. Quality control data for total metal analyses.

Quality parameter	Al	Cr	Cu	Fe	Mn	Ni	Pb	Zn
Daily duplicates %RSD (range)	0.8-4.6	1.2-6.2	0.4-6.0	0.4-5.1	0.2-6.6	0.8-9.2	1.1-8.2	0.5-4.0
Daily duplicates %RSD (average)	2.3	3.6	3.4	1.3	1.5	3.4	3.8	1.9
%RSD for PACS reproducibility (n=15)	6.2	8.3	3.2	2.6	7.4	9.7	6.2	4.0
Accuracy (% Recovery range)	85-106	84-114	87-96	86-95	85-113	85-115	86-109	86-99
Accuracy (%Recovery average)	96	96	91	89	99	101	95	91

Table A2. The ratios of eight heavy metals to Al in surface and deeper layer sediments of the collected cores. In cases of coarse-grained sediment cores MOT13A, MOT16, UN4, the ratios in fine sediment fraction (f < 63 μm) are calculated.

Core	Layer (cm)	Cr 10^4 Al^{-1}	Ni 10^4 Al^{-1}	Fe Al^{-1}	Mn 10^4 Al^{-1}	Cu 10^4 Al^{-1}	Pb 10^4 Al^{-1}	Zn 10^4 Al^{-1}
MOT 13 A	0-1	616	389	1.99	451	17.3	24.7	46.9
	10-12	277	261	1.44	303	12.4	15.4	30.4
MOT 16A	0-1	104	139	0.86	214	8.35	7.55	17.9
	30-32	85.0	127	0.87	187	7.35	9.35	14.7
UN 5	0-1	61.0	93.1	0.78	194	8.39	13.1	22.8
	30-32	58.9	84.5	0.77	137	6.85	6.52	15.2
MOT 16	0-1	170	174	1.19	244	10.4	12.9	24.8
	18-20	146	168	1.25	203	7.11	3.81	17.0
UN6	0-1	32.7	58.4	0.63	220	8.48	12.2	21.3
	24-26	34.2	61.6	0.66	159	6.41	7.29	14.0
UN 6A	0-1	37.0	47.5	0.56	145	6.7	9.76	18.8
	22-24	39.0	50.6	0.58	124	6.14	9.38	14.2
UN 4	0-1	38.6	47.4	0.46	104	6.9	7.63	15.2
	20-22	35.7	50.5	0.54	115	4.75	3.80	12.7
UN11	0-1	26.1	42.0	0.59	719	9.1	11.7	20.2
	30-32	33.8	45.1	0.66	303	7.75	7.29	14.8

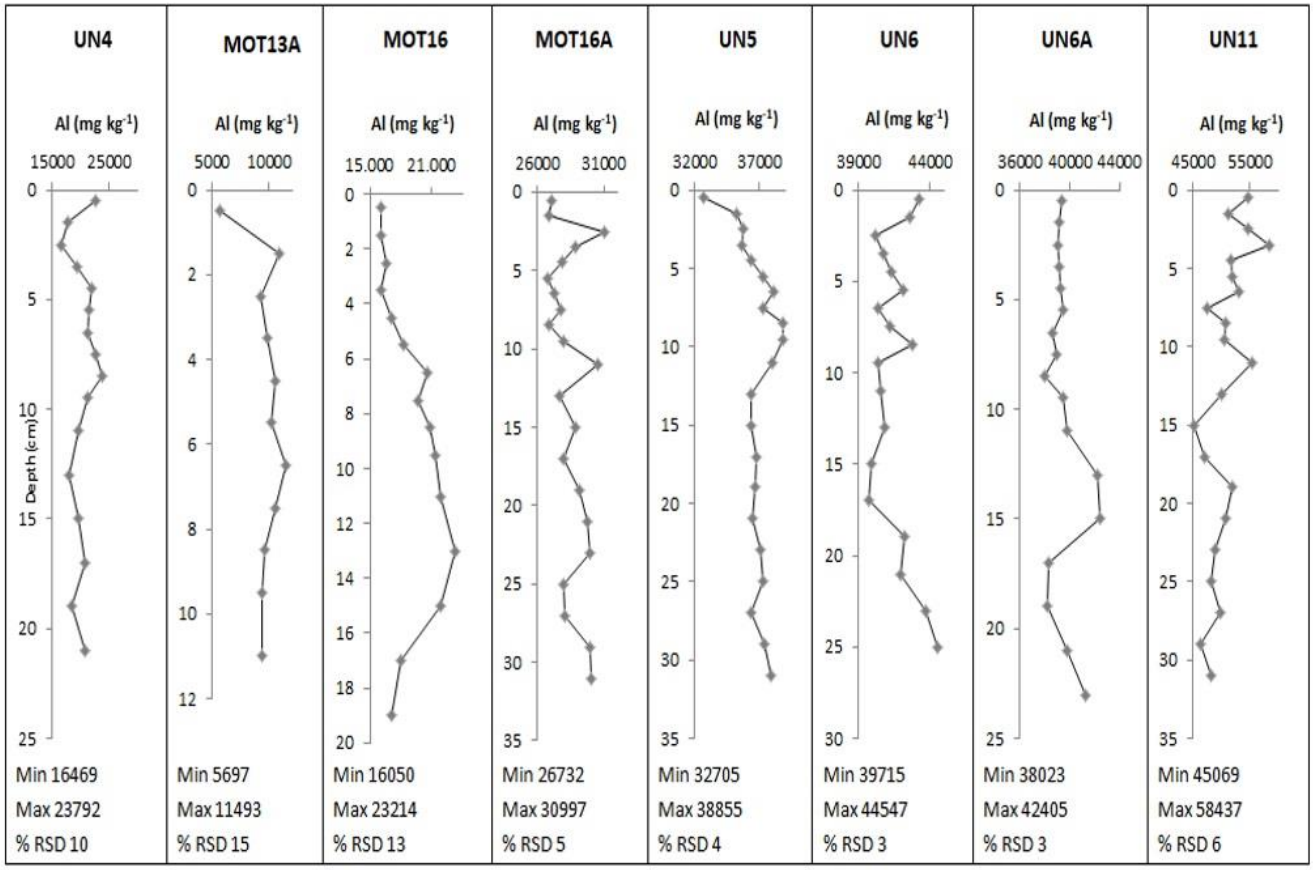

Figure A1: Vertical distributions of Al in mg kg $^{-1}$ in sediment cores. The concentrations in coarse cores MOT13A, MOT16, UN4 refer to the total sediment fraction (< 1 mm).

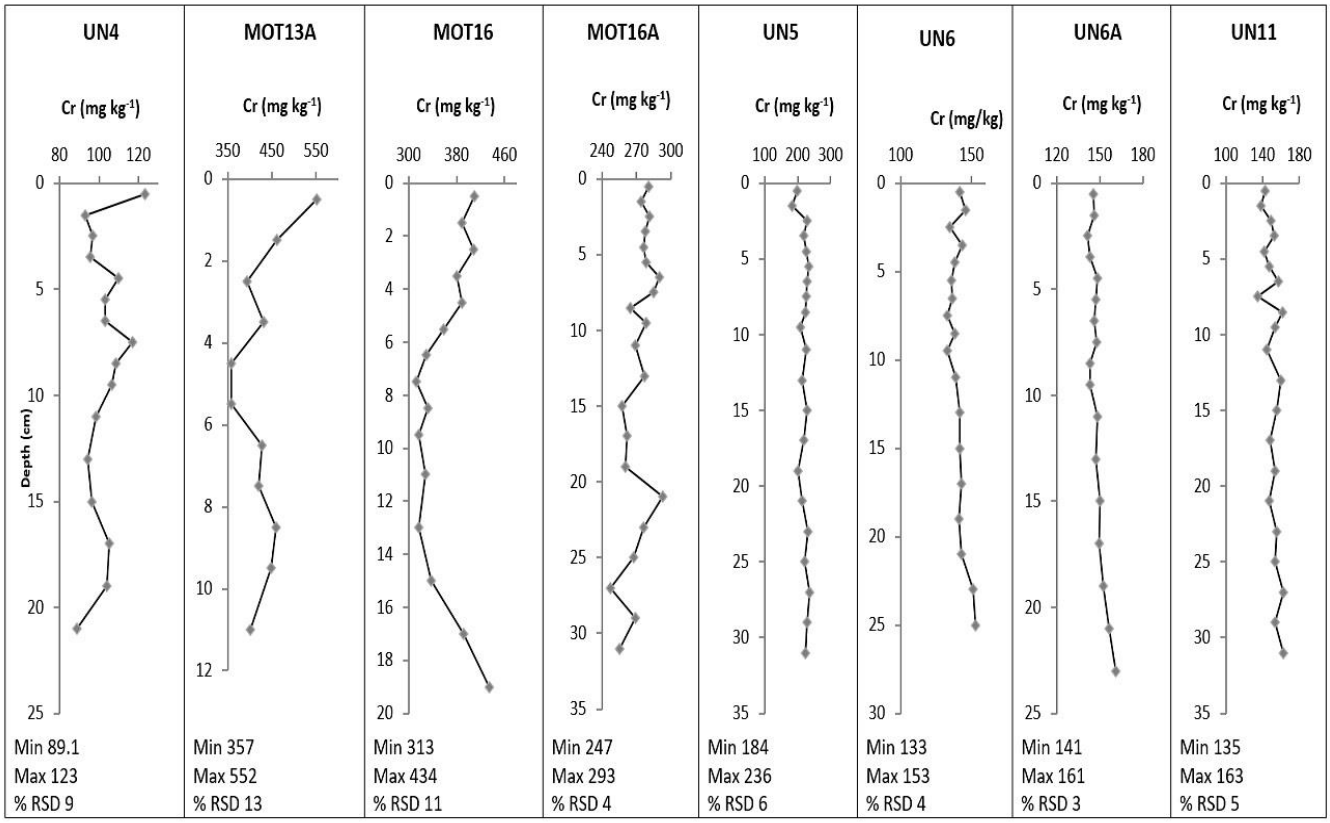

Figure A2: Vertical distributions of Cr in mg kg $^{-1}$ in sediment cores. The concentrations in coarse cores MOT13A, MOT16, UN4 refer to the total sediment fraction (< 1 mm).

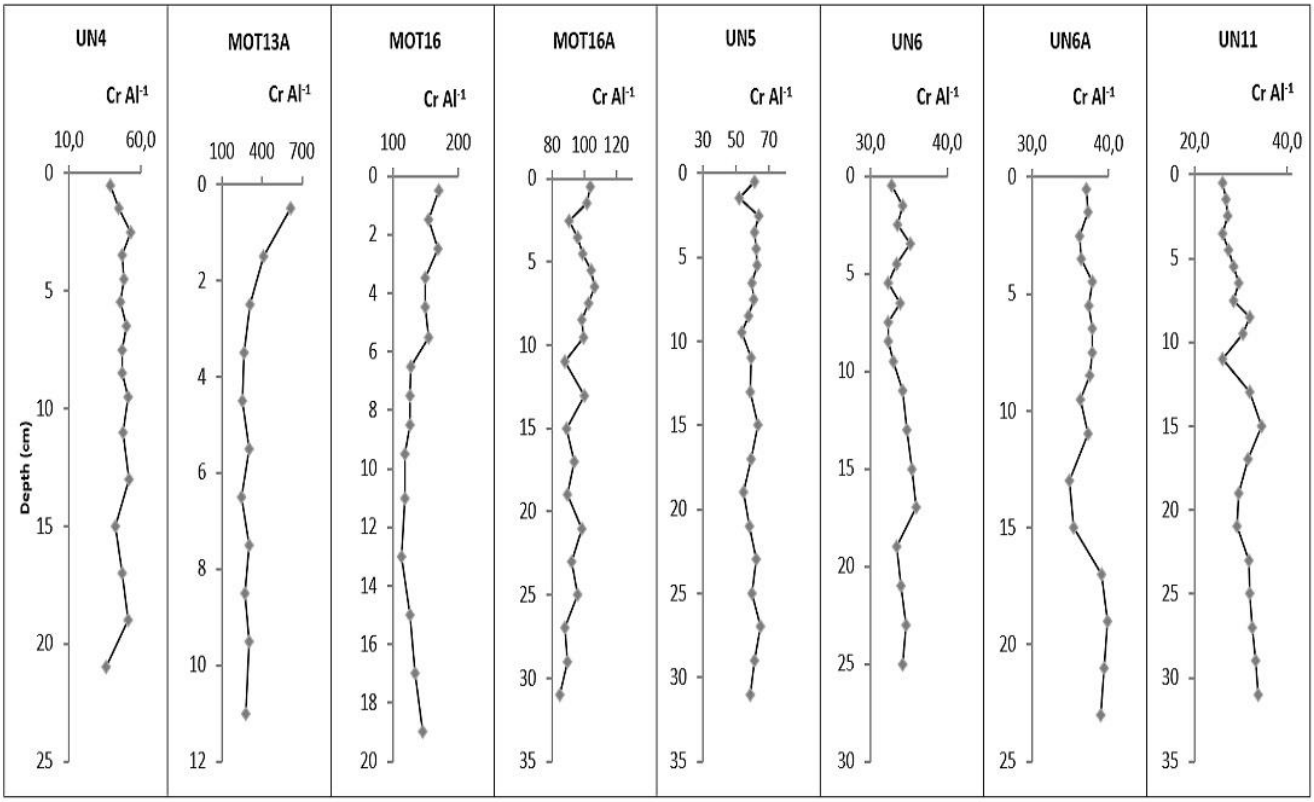

505

506 **Figure A3: Vertical distributions of Cr Al^{-1} × (10^4) in sediment cores. The ratios in coarse cores MOT13A, MOT16, UN4 are**
507 **calculated at the fine sediment fraction (< 63 µm).**

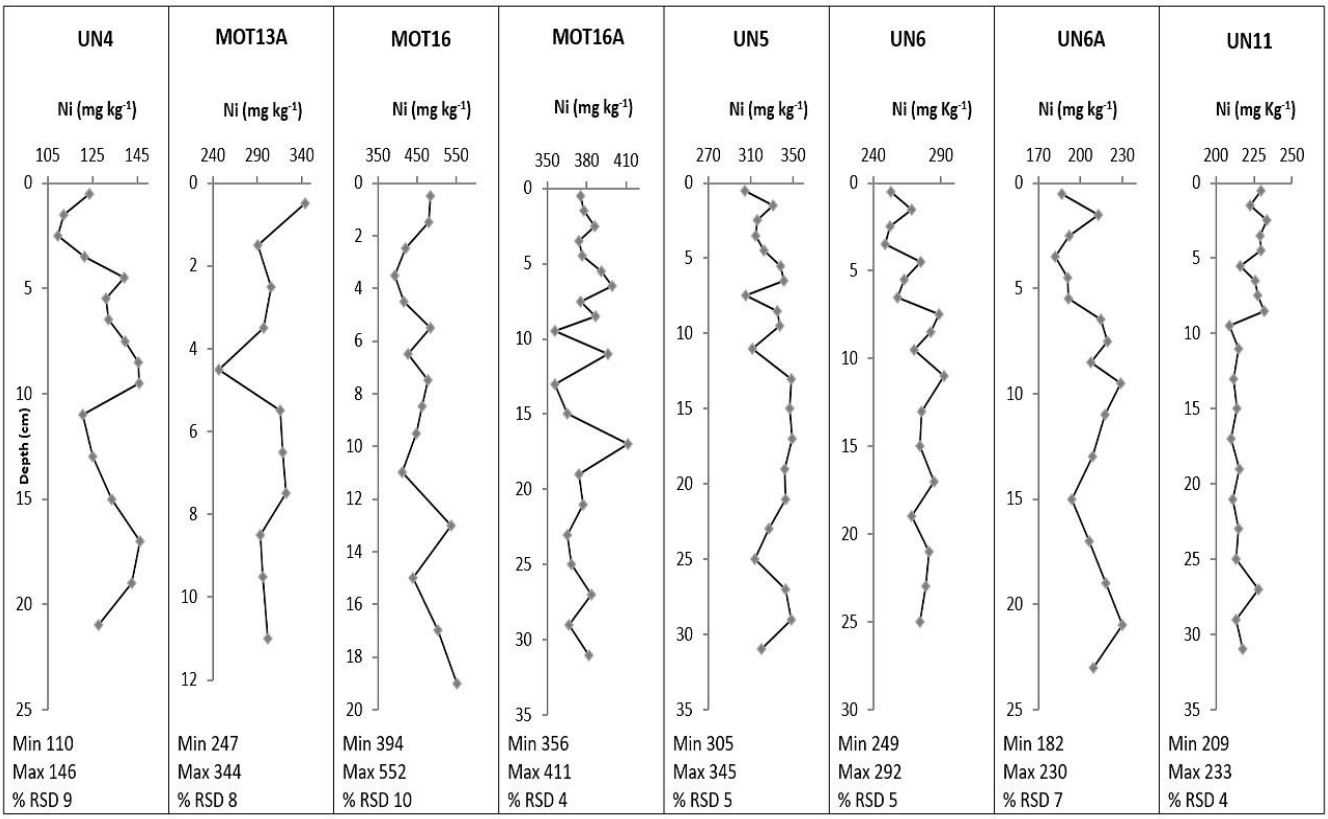

508

509 **Figure A4: Vertical distributions of Ni in mg kg^{-1} in sediment cores. The concentrations in coarse cores MOT13A, MOT16, UN4**
510 **refer to the total sediment fraction (< 1 mm).**

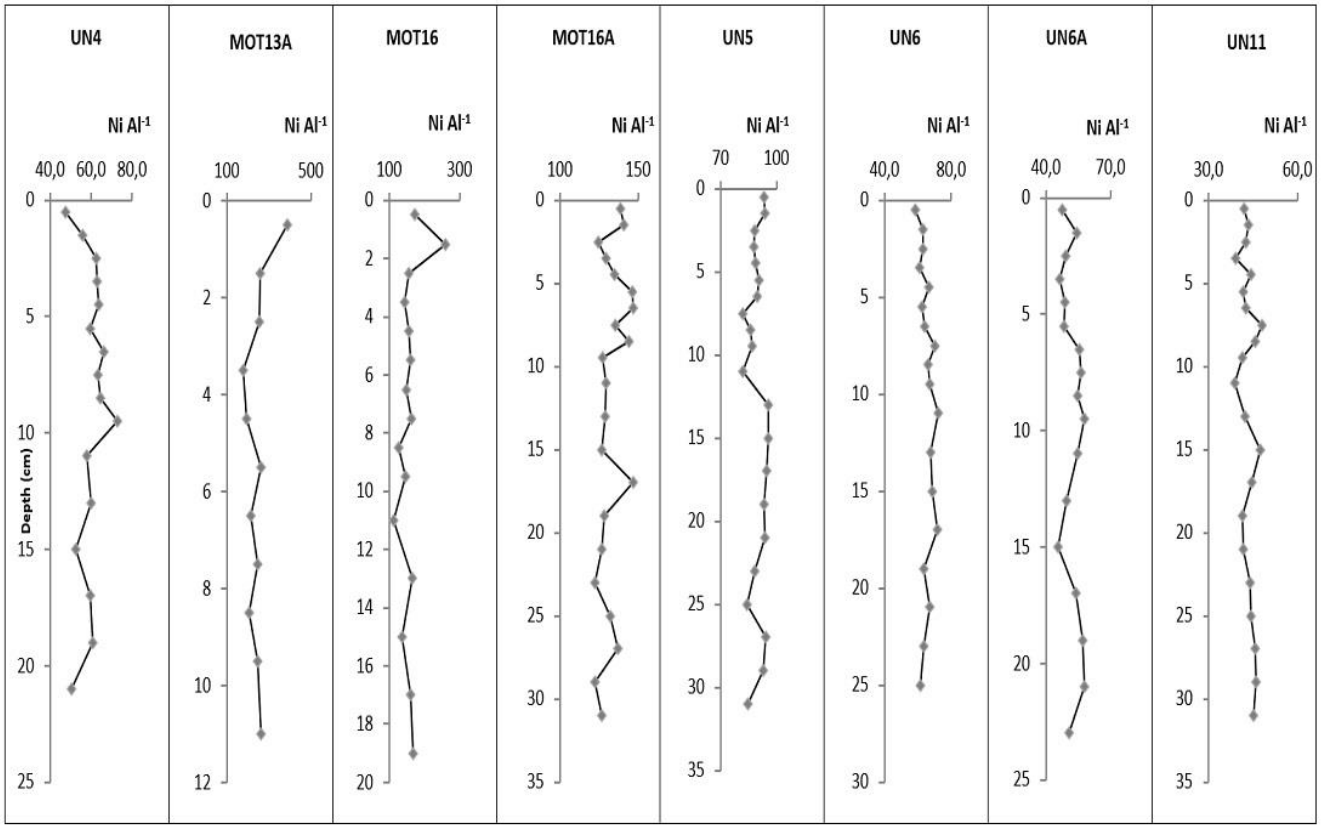

Figure A5: Vertical distributions of Ni Al^{-1} × (10^4) in sediment cores. The ratios in coarse cores MOT13A, MOT16, UN4 are calculated at the fine sediment fraction (< 63 µm).

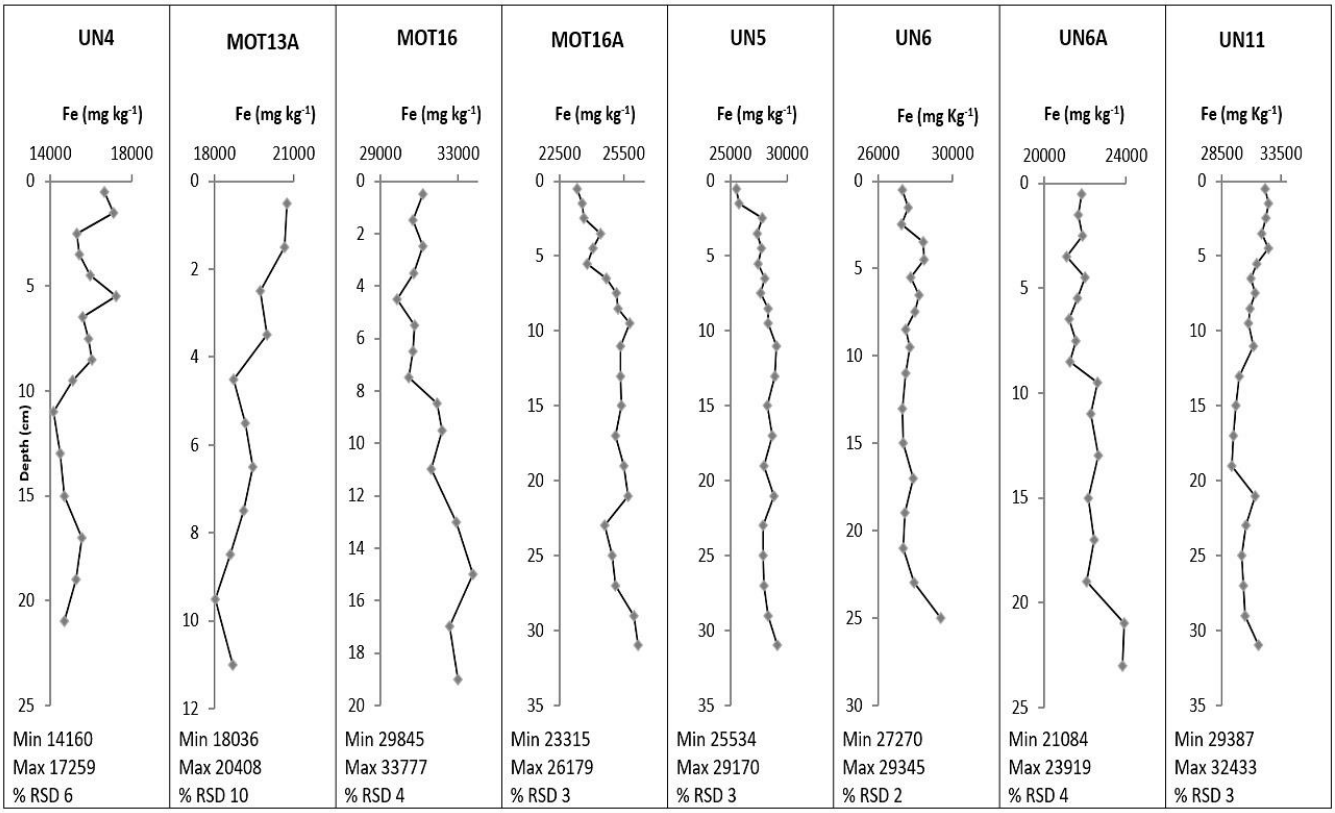

Figure A6: Vertical distributions of Fe in mg kg^{-1} in sediment cores. The concentrations in coarse cores MOT13A, MOT16, UN4 refer to the total sediment fraction (f < 1 mm).

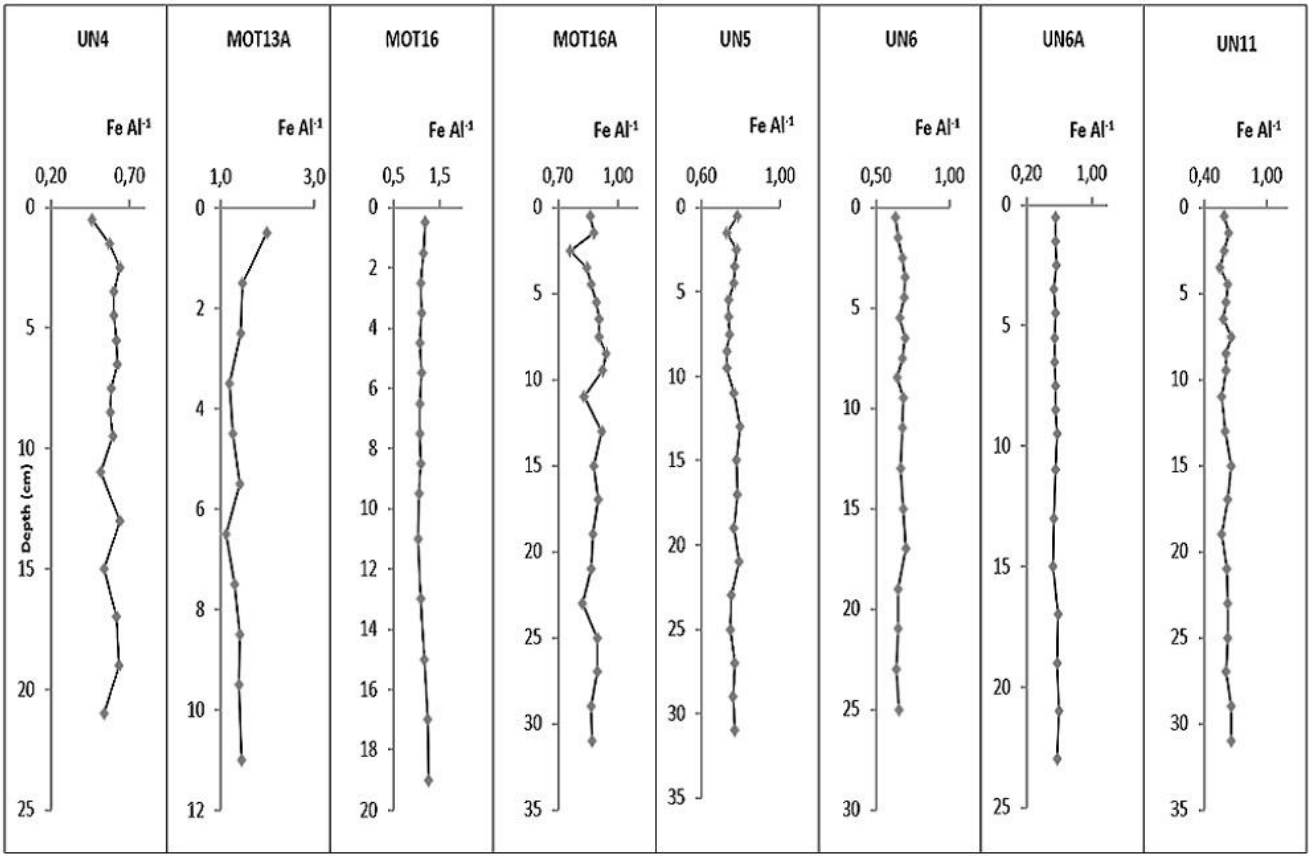

517

518 **Figure A7: Vertical distributions of Fe Al^{-1} in sediment cores. The ratios in coarse cores MOT13A, MOT16, UN4 are calculated at**
519 **the fine sediment fraction (< 63 µm).**

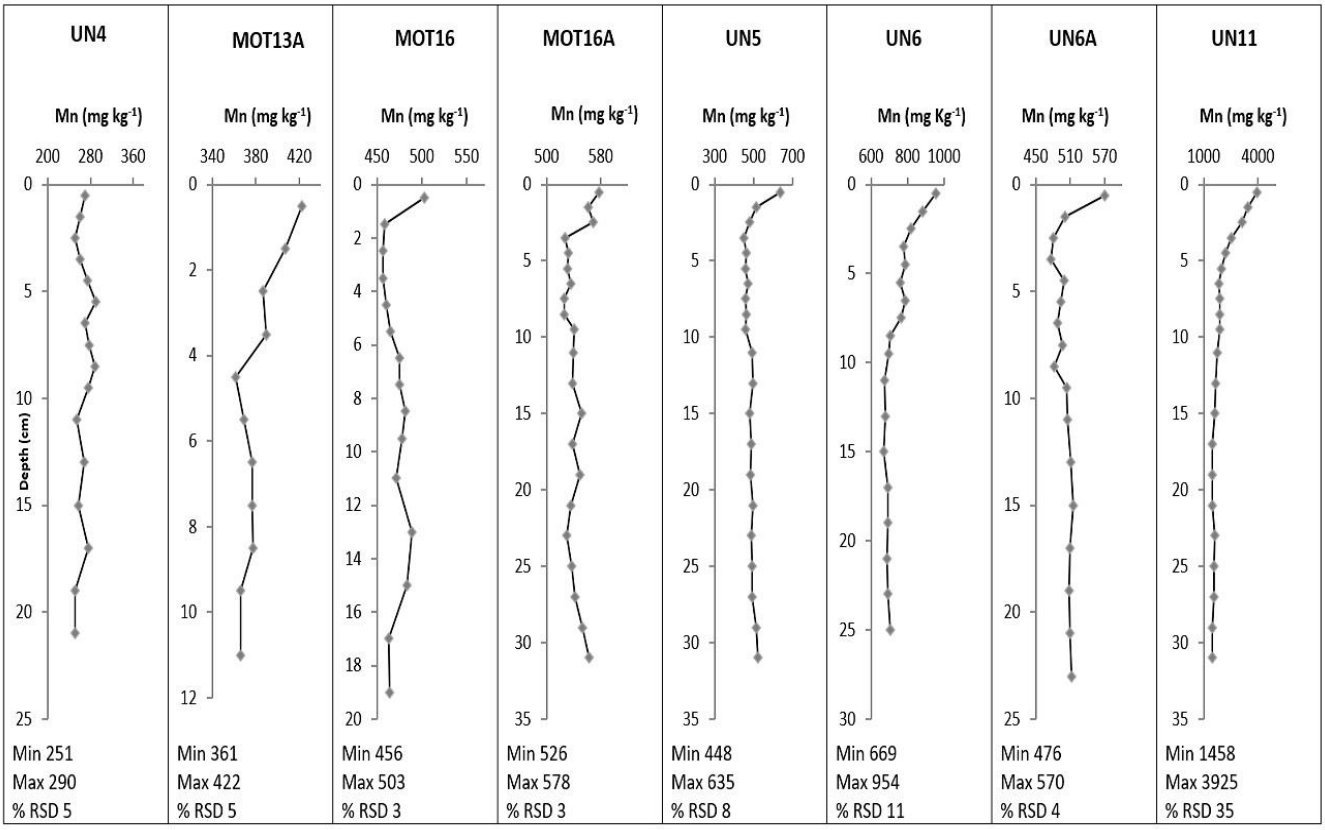

520

521 **Figure A8: Vertical distributions of Mn in mg kg^{-1} in sediment cores. The concentrations in coarse cores MOT13A, MOT16, UN4**
522 **refer to the total sediment fraction (< 1 mm).**

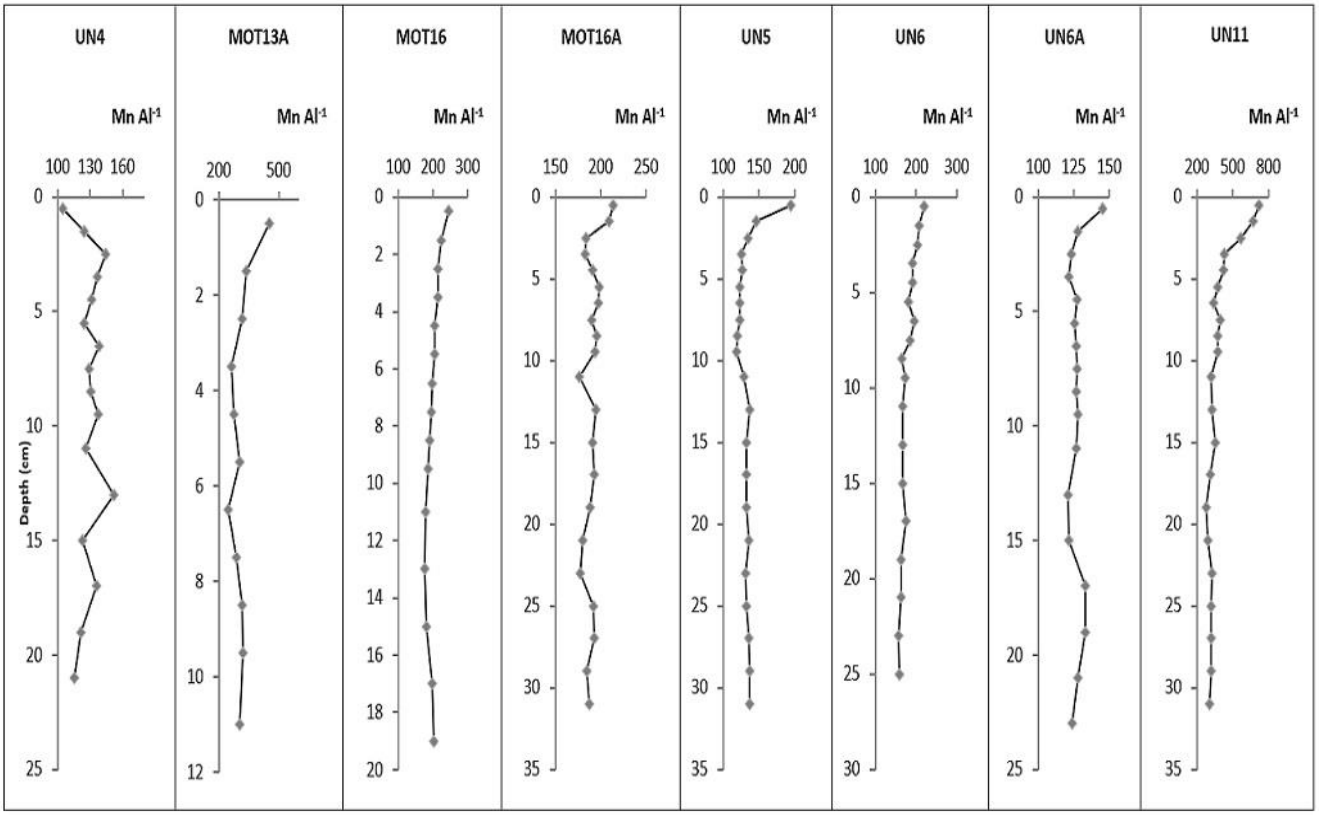

Figure A9: Vertical distributions of Mn Al^{-1}× (10^4) in sediment cores. The ratios in coarse cores MOT13A, MOT16, UN4 are calculated at the fine sediment fraction (< 63 µm).

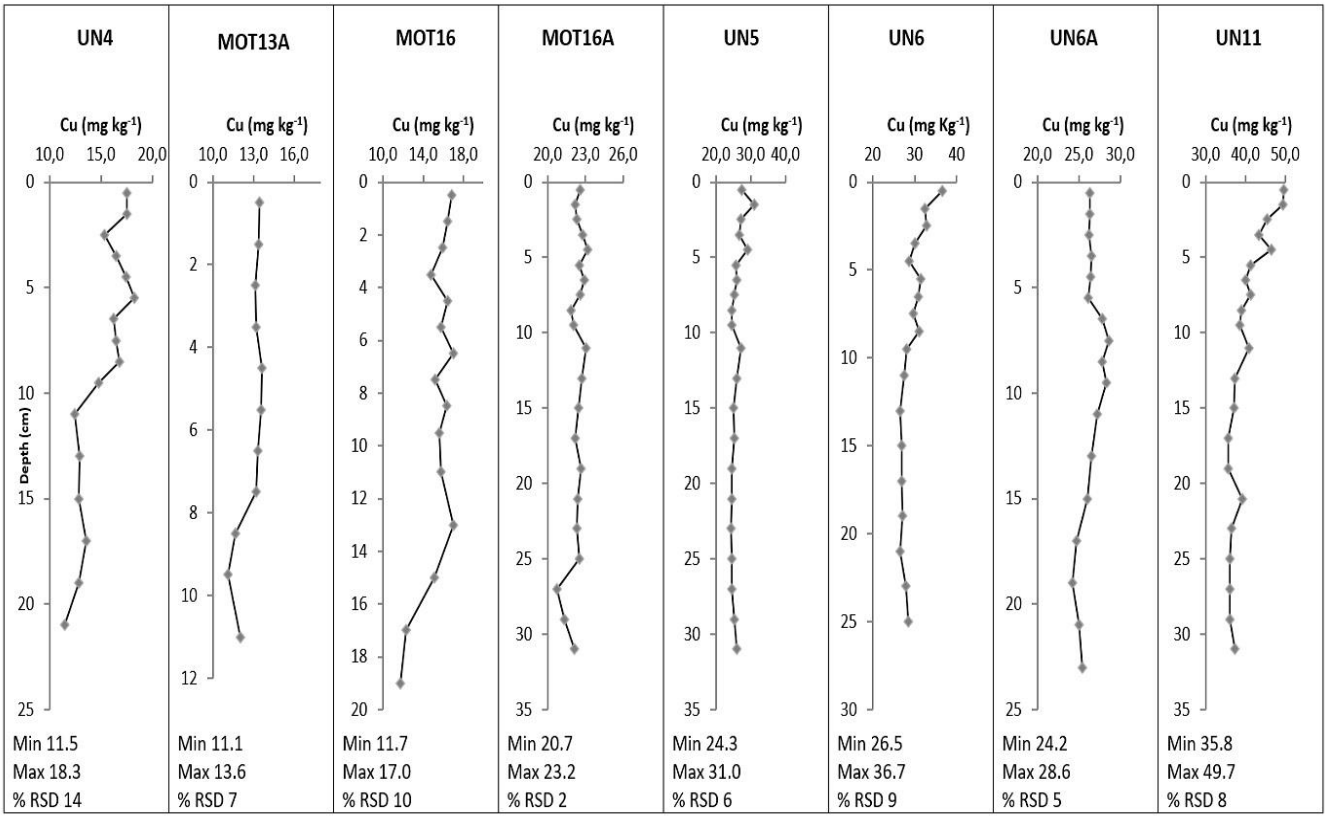

Figure A10: **Vertical distributions of Cu in mg kg^{-1} in sediment cores. The concentrations in coarse cores MOT13A, MOT16, UN4 refer to the total sediment fraction (< 1 mm).**

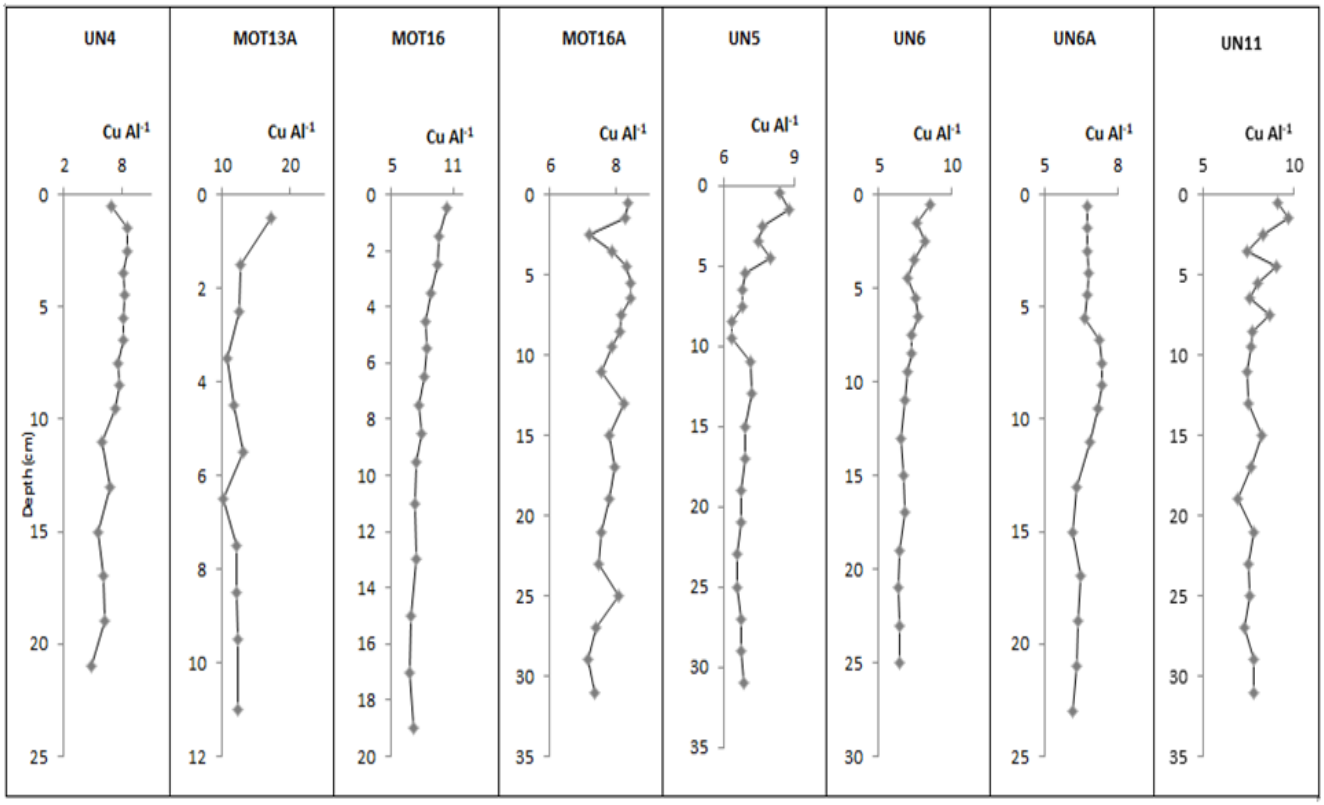

Figure A11: Vertical distributions of Cu Al^{-1} × (10^4) in sediment cores. The ratios in coarse cores MOT13A, MOT16, UN4 are calculated at the fine sediment fraction (< 63 µm).

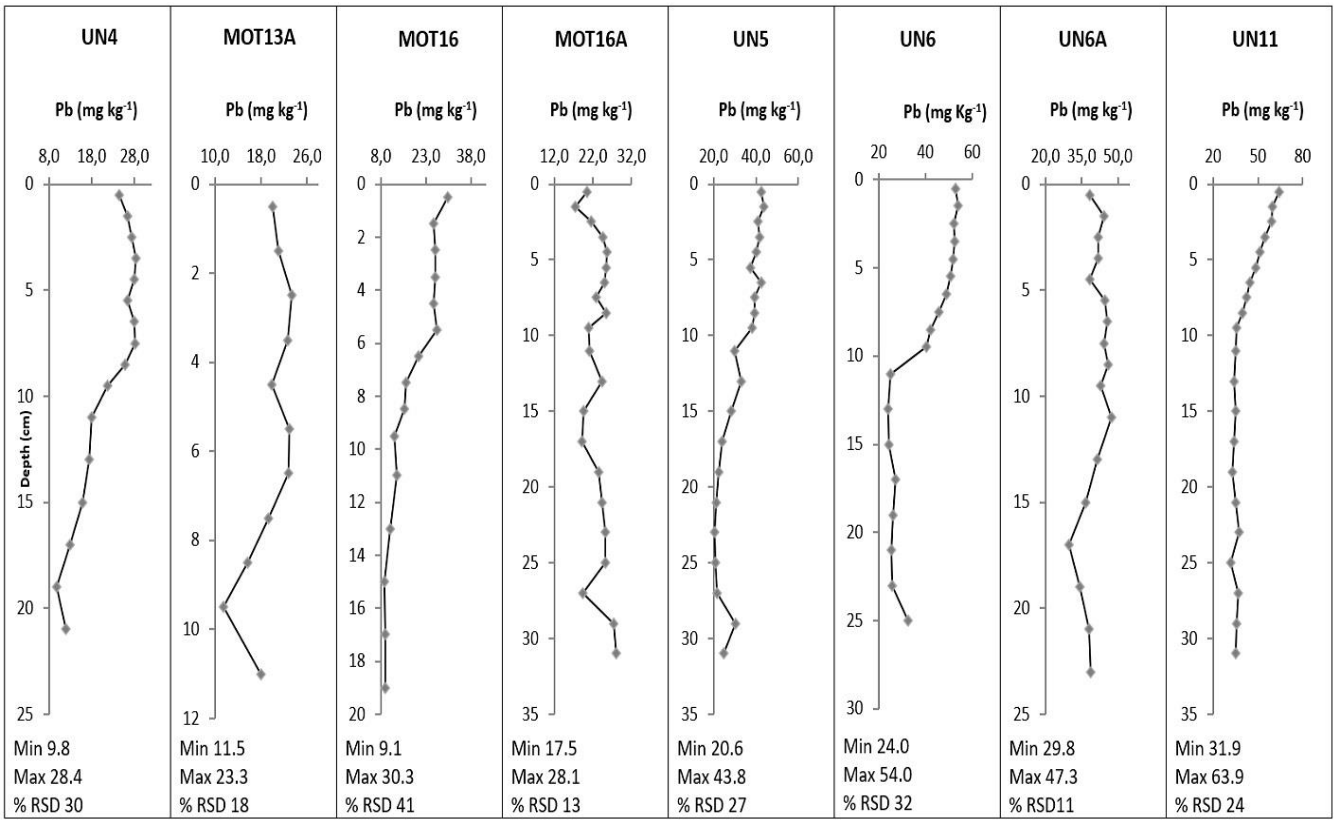

Figure A12: Vertical distributions of Pb in mg kg^{-1} in sediment cores. The concentrations in coarse cores MOT13A, MOT16, UN4 refer to the total sediment fraction (< 1 mm).

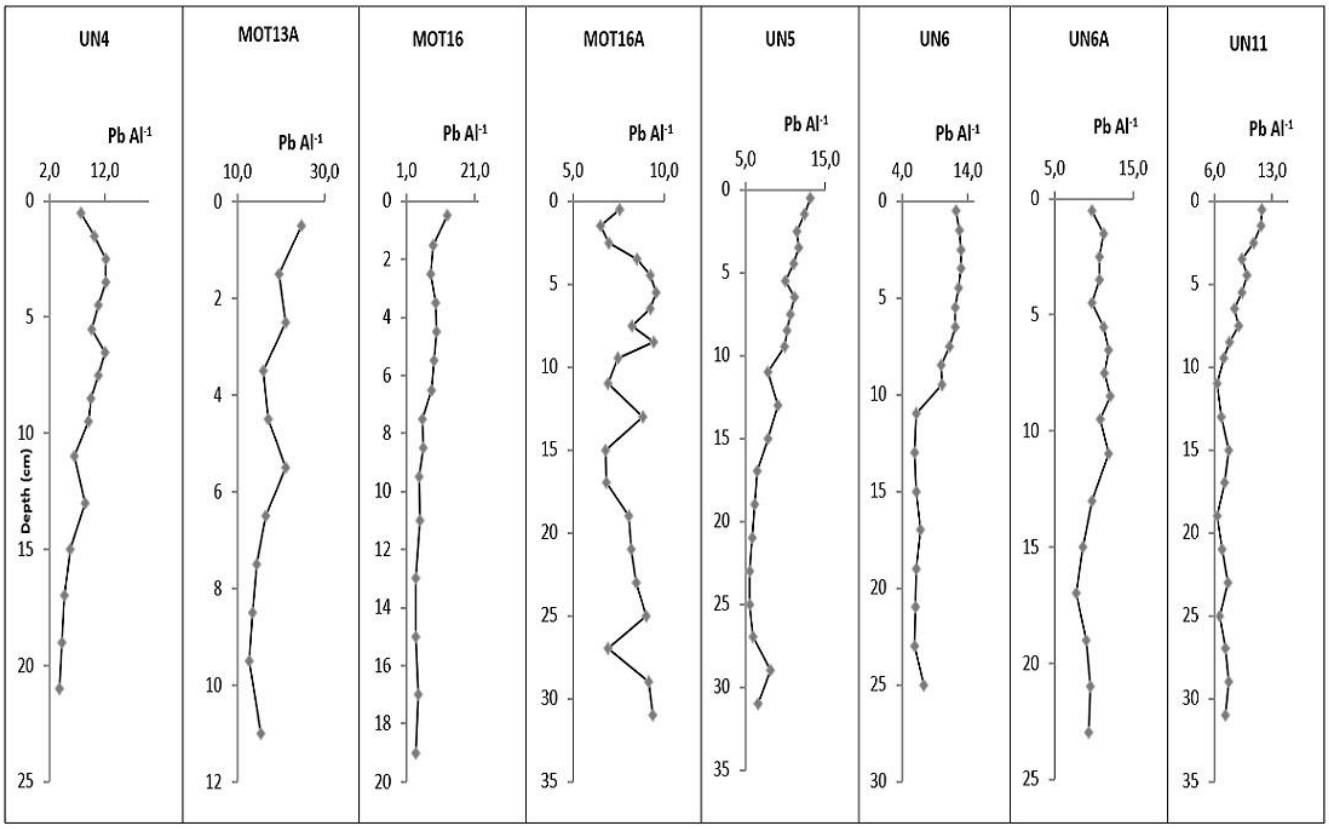

Figure A13: **Vertical distributions of Pb Al^{-1} × (10^4) in sediment cores. The ratios in coarse cores MOT13A, MOT16, UN4 are calculated at the fine sediment fraction (< 63 µm).**

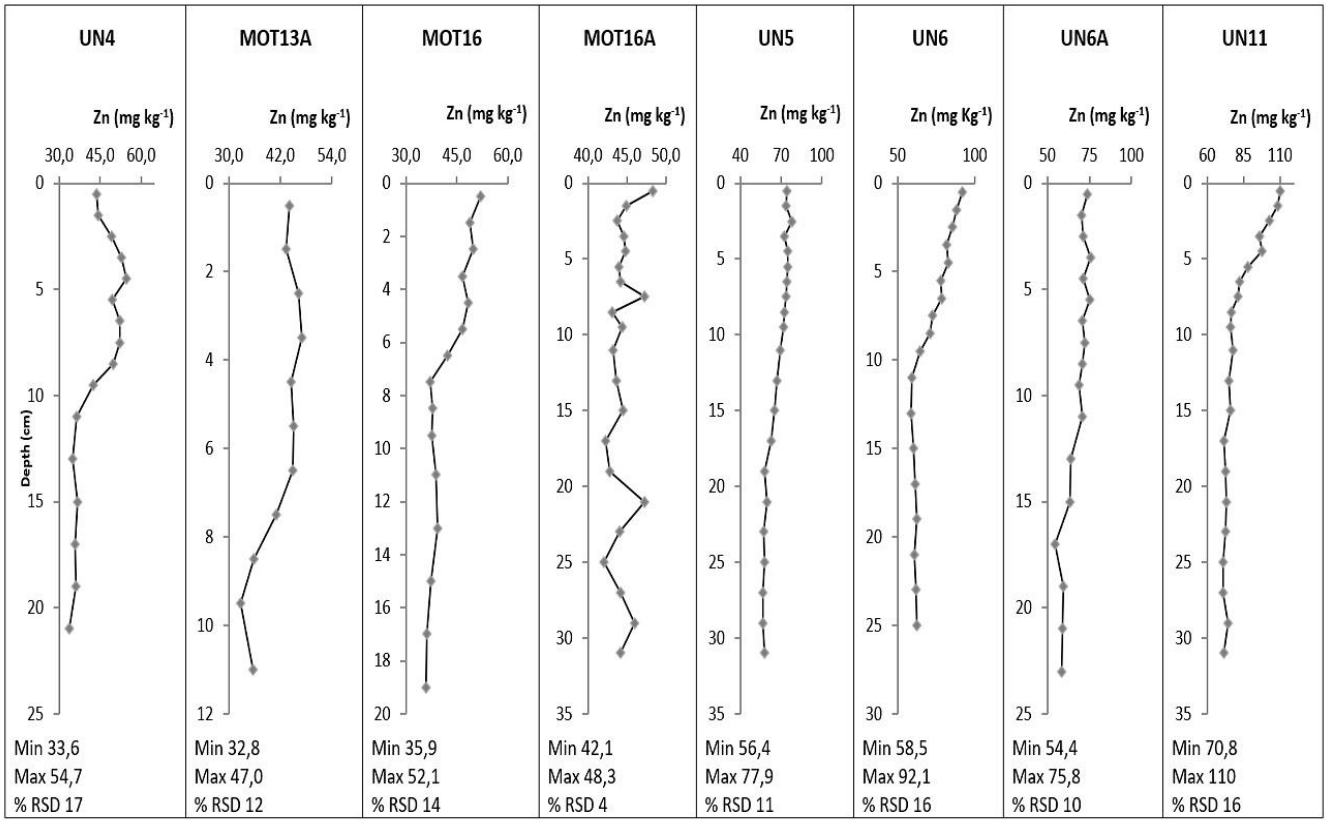

Figure A14: Vertical distributions of Zn in mg kg^{-1} in sediment cores. The concentrations in coarse cores MOT13A, MOT16, UN4 refer to the total sediment fraction (< 1 mm).

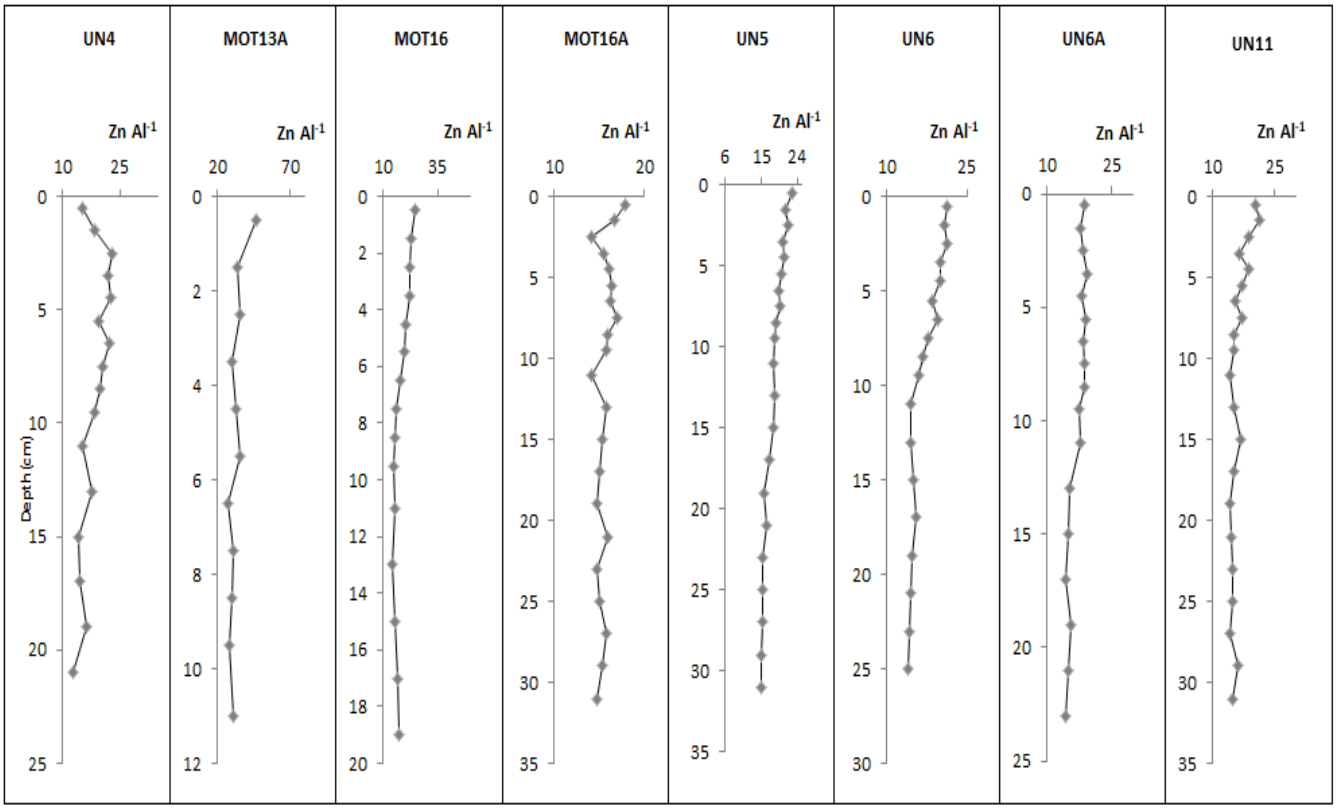

Figure A15: Vertical distributions of Zn Al^{-1} × (10^4) in sediment cores. The ratios in coarse cores MOT13A, MOT16, UN4 are calculated at the fine sediment fraction (< 63 µm).

Table A3. Spearman's correlation coefficient matrix for Al (mg Kg^{-1}), Cr (mg Kg^{-1}), Ni (mg Kg^{-1}), Fe (mg Kg^{-1}), Mn (mg Kg^{-1}), Cu (mg Kg^{-1}), Pb (mg Kg-1), Zn (mg Kg^{-1}), TOC (% Total Organic Carbon), carbonates (% $CaCO_3$) (N=140 sediment samples).

Correlations										
Spearman's rho	Al	Cr	Ni	Fe	Mn	Cu	Pb	Zn	TOC	% $CaCO_3$
Al	1.000									
Cr	-0.521**	1.000								
Ni	-0.453**	0.841**	1.000							
Fe	0.624**	0.081	0.179*	1.000						
Mn	0.735**	-0.108	0.029	0.694**	1.000					
Cu	0.924**	-0.419**	-0.342**	0.633**	0.746**	1.000				
Pb	0.676**	-0.440**	-0.433**	0.244**	0.397**	0.779**	1.000			
Zn	0.790**	-0.452**	-0.441**	0.459**	0.479**	0.882**	0.894**	1.000		
TOC	0.244**	-0.198*	-0.272**	0.096	0.155	0.351**	0.428**	0.483**	1.000	
% $CaCO_3$	-0.472**	-0.215*	-0.222**	-0.766**	-0.597**	-0.566**	-0.358**	-0.516**	-0.282**	1.000

**. Correlation is significant at the 0.01 level (2-tailed).

*. Correlation is significant at the 0.05 level (2-tailed).

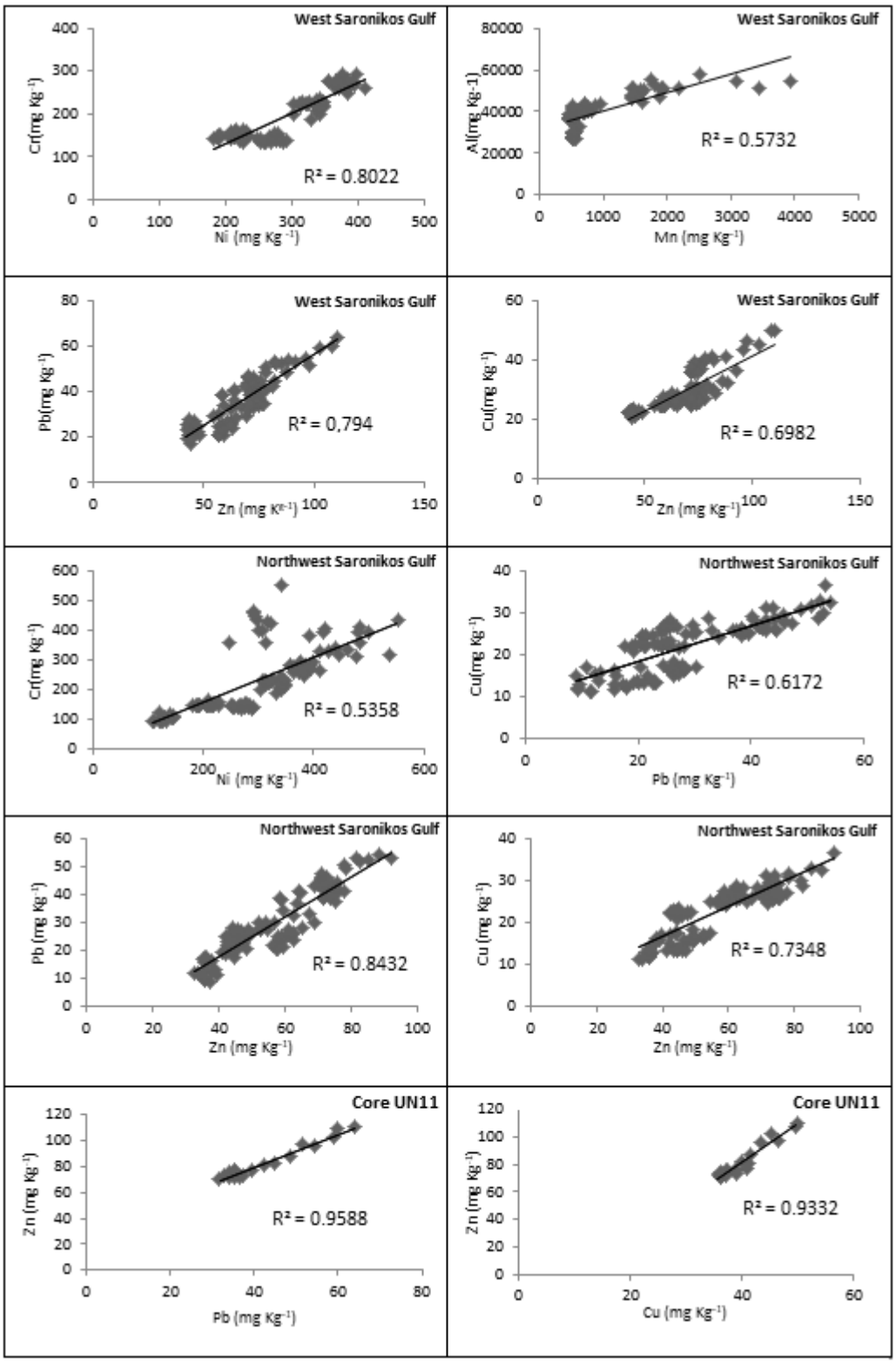

Figure A16: Correlations of heavy metals for the core samples of West Saronikos Gulf.

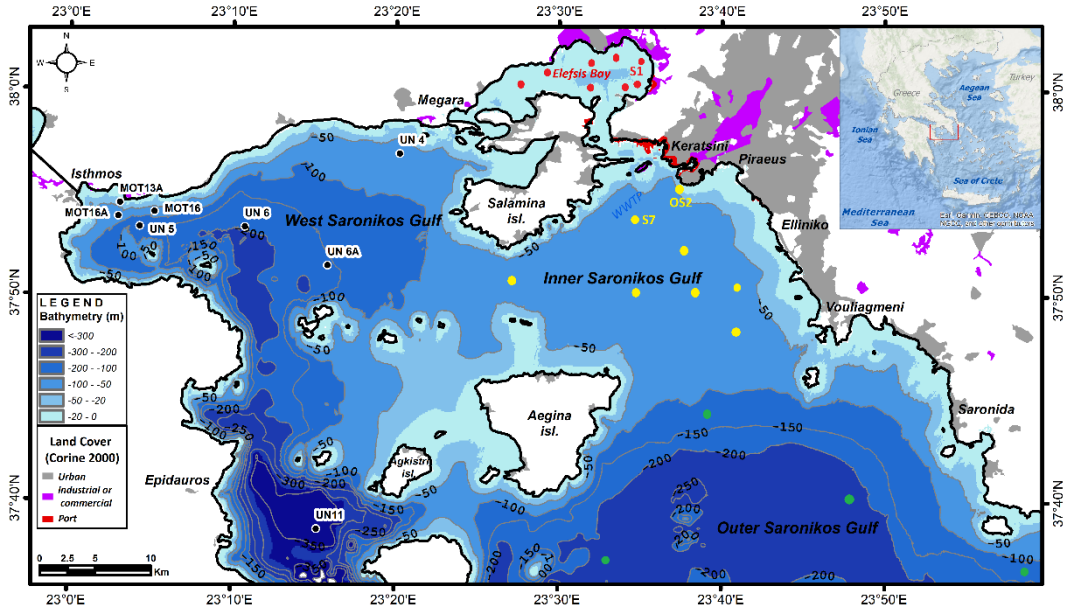

Figure A17: Map of Saronikos with stations in Elefsis Bay (red circles), Inner Saronikos (yellow circles) and Outer Saronikos (green circles) from which metal concentrations in sediments were review for the comparative discussion to the present study results in West Saronikos (black circles).

7 Data availability

Datasets and their sources are fully detailed in the manuscript.

8 Team list

Not applicable.

9 Author contribution

Georgia Filippi and Vasiliki Paraskevopoulou conducted the chemical analyses in the Laboratory of Environmental Chemistry of the National and Kapodistrian University of Athens. Georgia Filippi wrote the paper, with contributions and reviews from all co-authors. Konstantinos Lazogiannis constructed the map of the study area and contributed to compilation and improvements of figures. Manos Dassenakis was the supervisor of the laboratory work and this article.

10 Competing interests

The authors declare that they have no conflict of interest.

11 Special issue statement

The statement on a corresponding special issue will be included by Copernicus, if applicable.

12 Acknowledgements

We are grateful to the Hellenic Center for Marine Research (HCMR) and our colleagues Prof. S. Poulos, Dr Aik. Karditsa, and Dr F. Botsou for the assistance during the sampling. The research was funded by the European Union (European Social Fund) and National Funds (Hellenic General Secretariat for Research and Technology) in the framework of the project ARISTEIA I, 640 "Integrated Study of Trace Metals Biogeochemistry in the Coastal Marine Environment", within the "Lifelong Learning Programme". This project gave us the opportunity to reach the heavy metal pollution of West Saronikos Gulf. This paper summarizes the results of this study.

13 References

AOAC INTERNATIONAL: Appendix F: Guidelines for Standard Method Performance Requirements, AOAC Official Methods of Analysis, http://www.eoma.aoac.org/app_f.pdf, 2016.

Barjy, M., Maanan, M., Maanan, M., Salhi, F., Tnoumi, A., and Zourarah, B.: Contamination and environmental risk assessment of heavy metals in marine sediments from Tahaddart estuary (NW of Morocco), Hum. Ecol. Risk Assess., 26, 71-86, https://doi.org/10.1080/10807039.2018.1495056, 2020.

Bigus, P., Tobiszewski, M., and Namiesnik, J.: Historical records of organic pollutants in sediment cores, Mar. Poll. Bull., 78, 26-42, https://doi.org/10.1016/j.marpolbul.2013.11.008, 2014.

Chen, X., Li, S., Newby, S.M., Lyons, T.W., Wu, F., Owens, J.D.: Iron and manganese shuttle has no effect on sedimentary thallium and vanadium isotope signatures in Black Sea sediments, Geochim. Cosmochim. Ac., 317, 218233, https://doi.org/10.1016/j.gca.2021.11.010, 2022

Dassenakis, M., Scoullos, M., Rapti, K., Pavlidou., A., Tsorova, D., Paraskevopoulou, V., Rozi, E., Stamateli, A., and Siganos, M.: The distribution of copper in Saronicos Gulf after the operation of the wastewater treatment plant of Psitalia, Global Nest J., 5, 135-145, https://doi.org/10.30955/gnj.000282, 2003.

Diamantopoulou, A., Kalavrouziotis, I.K., and Varnavas, S.P.: Geochemical investigations regarding the variability of metal pollution in the Amvrakikos Bay Global Nest J., 21, 7-13, https://doi.org/10.30955/gnj.002733, 2019.

Gredilla, A., Stoichev., T., Fdez-Ortiz de Vallejuelo, S., Rodriguez-Iruretagoiena, A., Morais, P., Arana, G., and Madariaga, J.M.: Spatial distribution of some trace and major elements in sediments of the Cávado estuary (Esposende, Portugal), Mar. Poll. Bull., 99, 305–311, https://doi.org/10.1016/j.marpolbul.2015.07.040, 2015.

Hahladakis, J., Smaragnaki, E., Vasilaki, G., and Gidaragos, E.: Use of Sediment Quality Guidelines and pollution indicators for the assessment of heavy metal and PAH contamination in Greek surficial sea and lake sediments, Env. Mon. Assess., 185, 2843–2853, https://doi.org/10.1007/s10661-012-2754-2, 2012.

Jackson, M.L.: Soil Chemical Analysis, Soil Sci. Soc. Am. J., 22, 272-272, https://doi.org/10.2136/sssaj1958.03615995002200030025x, 1958.

Kanellopoulos, T., Kapetanaki, N., Karaouzas, I., Botsou, F., Mentzafou, A., Kaberi, H., Kapsimalis, V., and Karageorgis, A.: Trace element contamination status of surface marine sediments of Greece: an assessment based on two decades (2001–2021) of data, Environ. Sci. Pollut. R., 29, 45171-45189, https://doi.org/10.1007/s11356-022-20224-y, 2022.

Karageorgis, A.P., Kaberi, H., Price, N.B., Muir, G.K.P., Pates, J.M., and Lykousis, V.: Chemical composition of short sediment cores from Thermaikos Gulf (Eastern Mediterranean): Sediment accumulation rates, trawling and winnowing effects, Cont. Shelf Res., 25, 2456–2475, https://doi.org/10.1016/j.csr.2005.08.006, 2005.

649 Karageorgis, A.P., Botsou, F., Kaberi, H., and Iliakis, H.: Geochemistry of major and trace elements in surface sediments of
650 the Saronikos Gulf (Greece): Assessment of contamination between 1999 and 2018, Sci. Total Environ., 717, 137046,
651 https://doi.org/10.1016/j.scitotenv.2020.137046, 2020.
652
653 Karageorgis, A.P., Botsou, F., Kaberi, H., and Iliakis, H.: Dataset on the major and trace elements contents and contamination
654 in the sediments of Saronikos Gulf and Elefsis Bay, Greece, Data in brief, Sci. Total Environ., 29, 2352-3409,
655 https://doi.org/10.1016/j.dib.2020.105330, 2020a.
656
657 Kelepertsis, A., Alexakis, D., and Kita, I.: Environmental Geochemistry of soils and waters of Susaki Area, Korinthos, Greece,
658 Environ. Geochem. Hlth, 23, 117-135, https://doi.org/10.1023/A:1010904508981, 2001.
659
660 Kiratli, N., Ergin,M.: Partitioning of heavy metals in surface Black Sea sediments, Appl. Geochem., 11 (6), 775-788,
661 https://doi.org/10.1016/S0883-2927(96)00037-6, 1996
662
663 Kontoyiannis, H.: Observations on the circulation of the Saronikos Gulf: A Mediterranean embayment sea border of Athens,
664 J. Geophys. Res., 115, https://doi.org/10.1029/2008JC005026, 2010.
665
666 Long, E.R., MacDonald, D.D., Smith, S.L., and Calder, F.D.: Incidence of Adverse Biological Effects Within Ranges of
667 Chemical Concentrations in Marine and Estuarine Sediments, Environ. Manage., 19, 81-97,
668 https://doi.org/10.1007/BF02472006, 1995.
669
670 Loring, H.D., and Rantala, R.: Manual for the Geochemical Analyses of Marine Sediments and Suspended Particulate Matter.
671 Earth-Sci. Rev., 32, 235-283, http://dx.doi.org/10.1016/0012-8252(92)90001-A, 1992.
672
673 Manahan, E.: Water Chemistry, Green Science and Technology of Nature's Most Renewable Resource, 1st edition, CRC Press,
674 Taylor & Francis Group, U.S., 416 pp., 2011.
675
676 Nolting, R.F., Ramkema, A., and Everaarts, J.M.: The geochemistry of Cu, Cd, Zn, Ni and Pb in sediment cores from the
677 continental slope of the Banc d'Arguin (Mauritania), Cont. Shelf Res., 19, 665 -691, https://doi.org/10.1016/S0278-
678 4343(98)00109-5, 1999.
679
680 Ozturk, M.: Trends of trace metal (Mn, Fe, Co, Ni, Cu, Zn, Cd and Pb) distributions at the oxic-anoxic interface and in sulfidic
681 water of the Drammensfjord, Mar. Chem., 48, 329-342, https://doi.org/10.1016/0304-4203(95)92785-Q, 1995.
682
683 Panagiotoulias, I., Botsou, F., Kaberi, H., Karageorgis, A.P. and Scoullos, M.: Can we document if regulation and Best
684 Available Techniques (BAT) have any positive impact on the marine environment? A case based on a steel mill in Greece,
685 Environ. Monit. Assess., 189: 598, https://doi.org/10.1007/s10661-017-6324-5, 2017.
686
687 Panagopoulou, G., Heavy metals (Hg, Pb, Cd) at water samples and sediments of Saronikos Gulf, MSc thesis (in Greek),
688 University of Athens in Greece, Greece, 2018.
689
690 Paraskevopoulou, V.: Distribution and chemical behaviour of heavy metals in sea area affected by industrial pollution (NW
691 Saronikos), PhD Thesis in Chemical Oceanography (in Greek), University of Athens in Greece, Greece, 2009.

Paraskevopoulou, V., Zeri, C., Kaberi, H., Chalkiadaki, O., Krasakopoulou, E., Dassenakis, M., and Scoullos, M.: Trace metal variability, background levels and pollution status assessment in line with the water framework and Marine Strategy Framework EU Directives in the waters of a heavily impacted Mediterranean Gulf, Mar. Poll. Bull., 87, 323-337, https://doi.org/10.1016/j.marpolbul.2014.07.054, 2014.

Pavlidou, A., Kontoyiannis, H., and Psyllidou-Giouranovits, R.: Trophic conditions and stoichiometric nutrient balance in the Inner Saronicos Gulf (Central Aegean Sea) affected by the Psitalia seawage outfall, Fresenius Environ. Bull., 13, 12b., https://www.prt-parlar.de/download_feb_2004/, 2004.

Peña-Icart, M., Villanueva, M., Alonso Hernández, C., Rodríguez Hernández, J, Behar, M., and Pomares Alfonso, M.: Accepted Manuscript, Comparative Study of Digestion Methods EPA 3050B (HNO_3-H_2O_2-HCl) and ISO 11466.3 (aqua regia) for Cu, Ni and Pb Contamination Assessment in Marine Sediments, Mar. Env. R., 60-66, https://hal.archives-ouvertes.fr/hal-00720186/document, 2011.

Pohl, C., and Hennings, U.: The effect of redox processes on the partitioning of Cd, Pb, Cu, and Mn between dissolved and particulate phases in the Baltic Sea, Mar. Chem., 65, 41-53, https://doi.org/10.1016/S0304-4203(99)00009-2, 1999.

Prifti, E, Kaberi, H., Paraskevopoulou, V., Michalopoulos, P., Zeri, C., Iliakis, S., Dassenakis, M., and Scoullos, M.: Vertical distribution and chemical fractionation of heavy metals in dated sediment cores from the Saronikos Gulf, Greece, J. Mar. Sci. Eng., 10, 376, https://doi.org/10.3390/jmse10030376, 2022.

Psyllidou-Giouranovits R. and Pavlidou A.: Chemical characteristics in Catsiki V.A. (ed), Pollution research and Monitoring program in Saronikos gulf, Technical report, 1998 (in Greek).

Scoullos, M.: Lead in coastal sediments: The case of Elefsis gulf, Sci. Total Environ., 49, 199-219, https://doi.org/10.1016/0048-9697(86)90240-8, 1986.

Scoullos, M., Sakellari, A., Giannopoulou, K., Paraskevopoulou, V., and Dassenakis, M.: Dissolved and particulate trace metal levels in the Saronikos Gulf, Greece, in 2004. The impact of the primary Wastewater Treatment Plant of Psittalia, Desalination, 210, 98-109, https://doi.org/10.1016/j.desal.2006.05.036, 2007.

Skoog, D., Holler, F.J., and Nieman, T. A.: Principles of Instrumental Analysis, Fifth Edition, Saunders golden sunburst series, Saunders College Pub., Philadelphia , Orlando, Fla., Harcourt Brace College Publishers, 1998.

SoHelME, Papathanassiou, E. & Zenetos, A. (eds): State of the Hellenic Marine Environment., HCMR Publ., 360 pp, https://epublishing.ekt.gr/sites/ektpublishing/files/ebooks/Sohelme.pdf, 2005.

Sundby, B.: Transient state diagenesis in continental margin muds, Mar. Chem., 102 (1-2), 2-12, https://doi.org/10.1016/j.marchem.2005.09.016, 2006.

Sutherland, R.A.: Bed sediment-associated trace metals in an urban stream, Oahu, Hawaii, Env. Geol., 39, 611-627, https://doi.org/10.1007/s002540050473, 2000.

US EPA: Method 3050B Acid Digestion of sediments, sludges and soils, 1996, Revision 2, https://www.epa.gov/sites/default/files/2015-06/documents/epa-3050b.pdf, 1996.

Vrettou, E.: Heavy metals in sediment cores of Saronikos Gulf, MSc thesis (in Greek), University of Athens in Greece, Greece, 2019.

Walkley, A.: A Critical Examination of a Rapid Method for Determining Organic Carbon in Soils: Effect of Variations in Digestion Conditions and of Inorganic Soil Constituents. Soil Sc., 63, 251-264, http://dx.doi.org/10.1097/00010694-194704000-00001, 1947.

Xarlis, P.: Heavy metals (Cu, Ni, Zn) at water samples and sediments of Saronikos Gulf, MSc thesis (in Greek), University of Athens in Greece, Greece, 2018.